EIC Detector R&D Progress Report:
from July 2014 to December 2014

Project Name: eRD6, Proposal for detector R&D towards an EIC detector

Project Leader:

Brookhaven National Lab: Craig Woody
Florida Tech: Marcus Hohlmann
Stony Brook University: Klaus Dehmelt, Thomas Hemmick
University of Virginia: Kondo Gnanvo, Nilanga Liyanage
Yale University: Richard Majka

Date: January 01, 2015

Past

What was planned for this period?

Brookhaven National Lab:

Our effort during the period from July-December 2014 was divided in two main areas. The first was on the analysis of the test beam data taken at Fermilab in February of 2014 with our Minidrift GEM detector, and the second was on the design of the TPC/Cherenkov prototype detector, the acquisition of its components, and the start of its construction. The analysis of the test beam data with the Minidrift detector focused on the data taken using a readout plane with 2x10 mm chevron pads, which is the same type of readout plane we plan to use with the TPC/Cherenkov prototype. This also involved some additional lab measurements using a collimated X-ray source to study the intrinsic resolution properties of this type of readout which could be used to correct the data taken during the beam test. A new algorithm was developed for the chevron data using a time sliced vector finding procedure that produced a resolution comparable to what was obtained with much finer pitched strips using a COMPASS style readout (~ 100 μm at small angles and increasing to ~ 200 μm at 30°). The design of the TPC/Cherenkov prototype is now essentially complete and many of the critical components, such as the field cage, readout board, and various electrical, mechanical and optical components are now in hand. The electrostatic simulation of the field cage was further developed using ANSYS and the field non-uniformities in the fiducial drift region were shown to be less than 0.1%. The field cage foil passed its initial high voltage test and an initial assembly of the main part of field cage has been completed. Additional tests of charge attachment in various types of gas mixtures were also performed.
The main objectives for this period were:

1. To complete the analysis of the Fermilab test beam data taken in February 2014 with the Minidrift GEM detector with the chevron pad readout plane.

2. To complete the design of the TPC/Cherenkov prototype detector, acquire its components, and begin its construction.

For objective 2, the design consists of both electrical and mechanical components and involves some very challenging features. The use of the photosensitive GEM requires that one side of the field cage be optically transparent, which requires an array of fine wires, and that the GEM be brought in close proximity to the field cage, which causes some very high field gradients. In addition, since the photosensitive

GEM is coated with CsI and there is no window between it and the TPC, the entire detector must be assembled and kept in an inert atmosphere at all times.

Florida Tech:

We planned to continue analyzing forward tracking data taken at the Fermilab beam test in Oct 2013. Specifically, we wanted to improve the angular resolution for the large GEM prototype detector with radial zigzag strip readout with a better non-linear response correction. We planned to submit a NIM A paper once this analysis is done. The other main objective was to work, together with the U. Virginia group and Bernd Surrow and others from another EIC RD group, on designing and constructing the next full-size EIC GEM prototype for forward tracking using domestically sourced GEM foils and other materials.

Stony Brook University:

It was planned that the results of the two test-beam campaigns were to be written up for publication in a peer-reviewed journal.
The RICH prototype showed limited position resolution in the past test-beam campaigns and for overcoming the limitation we proposed to work on a resistive charge division scheme in terms of simulating and testing with appropriate readout boards. It is hoped that this allows high precision single photon position resolution measurements.
After simulating and deciding for a reasonable readout scheme it is planned to prepare a suitable readout board with proper resistive anode layer and readout pads and the performance to be tested and verified with a radiation source that can be positioned relative to the readout board with high precision.

University of Virginia:
For the period from June 2014 to December 2014, we planned to explore new ideas around four main focus points in order to improve the design, the assembly and the performances of a 1 m long EIC-specific Triple-GEM prototype.
Light-weight – low-mass GEM:
We want to replace the honeycomb support of the flexible 2D readout board of the GEM detector by a gas volume with 25 μm Kapton foil window. The gas volume is also used to contra balance the overpressure inside the detector.
New assembly technique:
The second idea that we planned to investigate is to build triple-GEM detector in which the frames supporting the GEM foils are not glued together but stacked and kept close with plastic screws and O-ring for gas tightness. The technique offers the double advantage of low-mass detector and the possibility to re-open the chamber to replace parts of the detector such as bad GEM foils if needed.
2D stereo angle (u/v) EIC-specific readout board:
We propose a design upgrade of the 2D u/v readout board that was used for the first EIC GEM prototype. Unlike the current readout board, the new one will have all front end electronics located at the outer radius of the chamber in order to reduce the dead area on the sides and the material at the inner radius close to the beam pipe.
Mini-drift capabilities of the u/v readout board:
We planned to collaborate with Craig Woody's group at BNL on the implementation of their work on the mini-drift onto large area GEM detector with u/v readout board. The goal here is to study the spatial resolution performance of the detector at large angle.
We also planned to form an active collaboration with Marcus Hohlmann group at Florida Tech (FIT) and Bernd Surrow group at Temple University to work on common EIC forward Tracker (FT) R&D project, and join the ongoing collaboration

with the US based Tech Etch company for a domestic production of such large size GEM foil.

Yale University:

3-Coordinate GEM
During the past period it was planned to refine the analysis of the Fermilab test beam data for the 800 μm pitch chambers and to do more detailed electrical testing for the 600 μm chambers.

Hybrid Gain Structure for TPC readout – 2 GEM plus Micromegas (2-GEM+MMG)
During this period it was planned to make measurements of the critical parameters (energy loss resolution, *dE/dX,* and Ion Back Flow (IBF)) varying voltages on the gain elements, varying transfer fields between the elements, and varying the working gas mix. Further it was planned to make stability measurements using a heavily ionizing source to study the sparking behavior. We also intended to study different fabrication techniques including using ridges in the gaps between readout plane elements to support the MMG (MMG) mesh so as to minimize possible gain variations due the presence of the support elements. Also we intended to study segmenting the MMG mesh to reduce the energy in a discharge.

What was achieved?

Brookhaven National Lab:

Minidrift Detector

We have now essentially completed the analysis of all the data taken with the Minidrift GEM detector with the chevron readout plane. These results were presented at the 2014 IEEE Nuclear Science Symposium in November and will soon be submitted for publication in the IEEE Transactions on Nuclear Science along with the complete set of results from the Minidrift GEM detector.
Figure 1 shows the Minidrift detector in the MT6.1 test beam area at Fermilab and the silicon telescope that was used to provide precise beam track information. Figure 2 shows the chevron readout board. The readout consisted of 2x10 mm^2 chevron pads and was divided into four quadrants with four different chevron patterns. Only one quadrant with a fine (0.5 mm) pitch was tested.

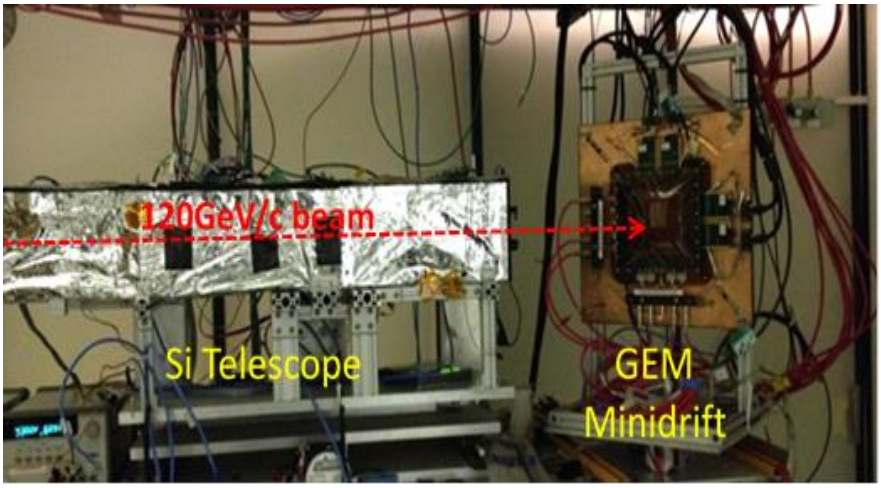

Figure 1 Setup in the Fermilab test beam with the Minidrift GEM detector and the silicon telescope used to measure beam tracks.

For the chevron pad readout with a 2x10 mm^2 pad size, a simple centroid algorithm cannot provide precise position information for any appreciable angle since it relies on the localized charge spread over a single pad to interpolate the position within

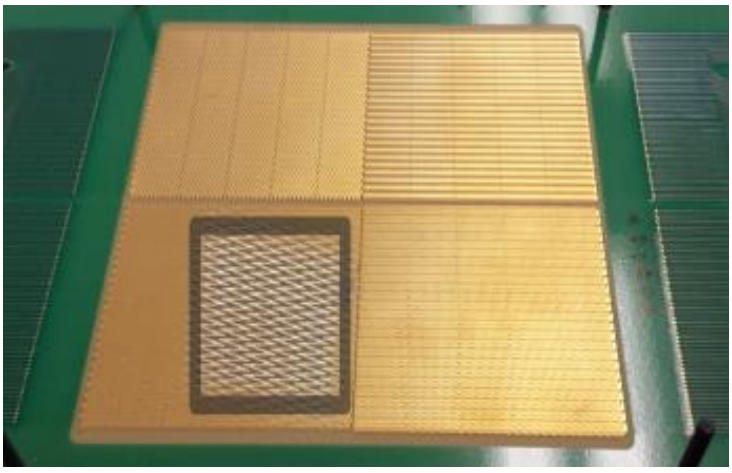

Figure 2 Chevron readout board showing a detail of the fine pitched chevrons in the region that was measured.

a pad, and tracks at large angles deposit charge on many pads and are subject to

large fluctuations. Therefore, new algorithm was developed that divided the data into 25 ns time slices that sampled the charge spread over a very limited region in the drift direction, and therefore allowed a centroid determination using just a few pads at a time. These centroid measurements were then combined to form a vector along the drift direction, which then allowed a determination of both the position and the angle of the track.

Figure 3 shows the position resolution derived from the chevron pad readout plane. The blue points are with the time sliced vector algorithm, both uncorrected and

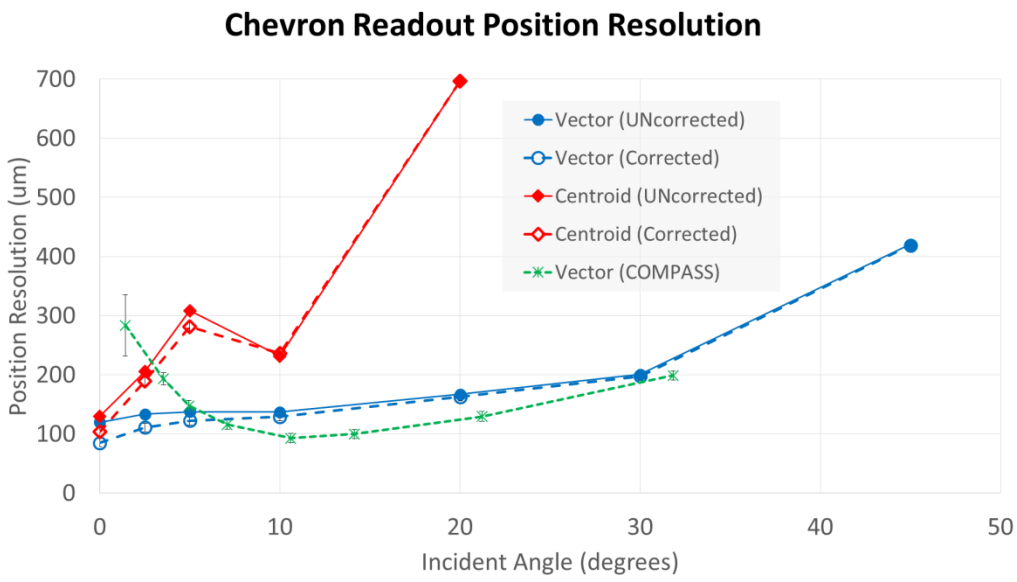

Figure 3 Position resolution derived from the chevron pad readout plane with the Minidrift GEM detector. Blue curves are for the time sliced vector algorithm and red curves are for a simple centroid calculation. Also shown is data with the COMPASS readout plane using a different vector reconstruction algorithm for comparison.

after applying a correction for the intrinsic differential non-linearity of the chevron board measured in the lab using a collimated X-Ray source. Also shown in green is data with the COMPASS style readout board using a different vector reconstruction algorithm. For the chevron case, the position resolution is below 100 μm at zero degrees, and increases to ~ 200 μm at 30°. The time sliced vector algorithm is clearly superior to the one used for the COMPASS board at small angles. Also shown is the position resolution for the chevron pads using a simple centroid algorithm, which works only at very small angles. The dip at 10° we believe is due to a geometrical effect when the charge begins to spread over more pads, improving the resolution at moderate angles, but then worsens again at larger angles due to fluctuations.

The vector reconstructed using the time sliced method also allows an angle determination of the track. Figure 4 shows the angular resolution obtained with the time sliced method compared with a different vector finding algorithm used with the COMPASS readout board. The angular resolution is slightly worse, but approaches ~ 20 mrad at large angles. Given the much coarser segmentation of the chevron pads relative to the COMPASS strips, this is most likely still acceptable in most applications.

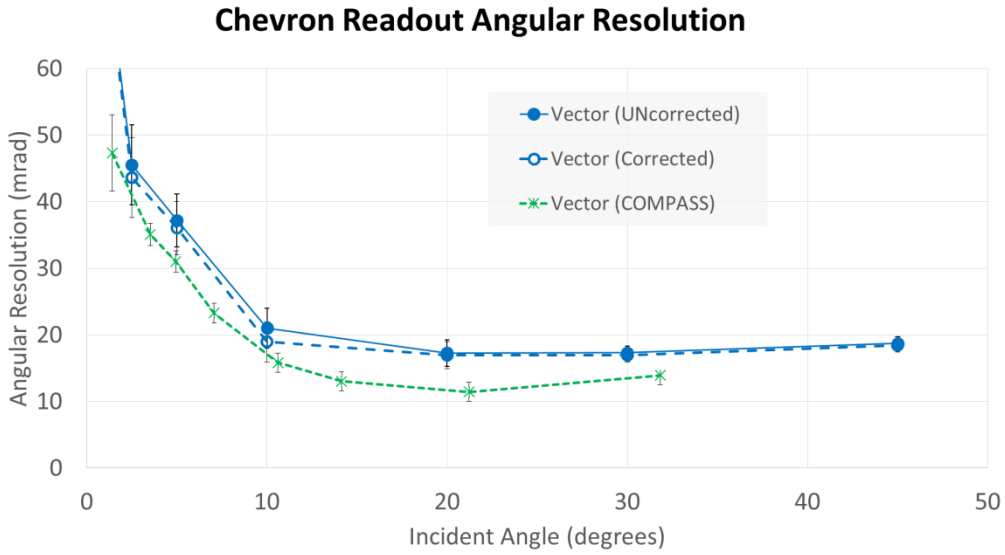

Figure 4 Angular resolution derived from the chevron pad readout plane with the Minidrift GEM detector. Blue curves are for the time sliced vector algorithm method. Also shown is data with the COMPASS readout plane using a different vector reconstruction algorithm for comparison.

TPC/Cherenkov Prototype Detector

The design of the TPC/Cherenkov prototype detector is essentially complete and many of its components are already in hand. The detector consists of a 10x10x10 cm^3 drift volume for the TPC where charge is drifted vertically downward to a 10x10 cm^2 GEM detector. In order to detect Cherenkov light, one side of the field cage must be optically transparent, which is formed using an array of fine wires. The remaining three sides of the field cage is formed using a kapton foil with copper strips. Initially only the TPC portion of the detector will be tested in order to insure that it is working and to understand its properties before introducing the Cherenkov detector. For this mode of operation, the fourth side of the field cage will be replaced with a kapton foil similar to the one used on the other three sides.
The uniformity of drift field was studied using the electrostatic package within the ANSYS simulation software. Figure 5 shows a result from the current simulation with the four sided kapton foil configuration. Figure 5, upper shows the deviation of the electric field vector from its nominal value along the drift direction as a function of position in a transverse plane at the center of the fiducial volume. Figure 5, lower shows the same deviation as a function of one of the transverse coordinates and the position along the drift direction. In all cases, the deviation is less than 0.1% at the limits of the fiducial volume and much less than that inside the fiducial volume. Additional simulations are currently under way to study what effect the wire array will have on the field uniformity, but we expect that this will only affect the exit region of the drift volume just in front of the photosensitive GEM detector.

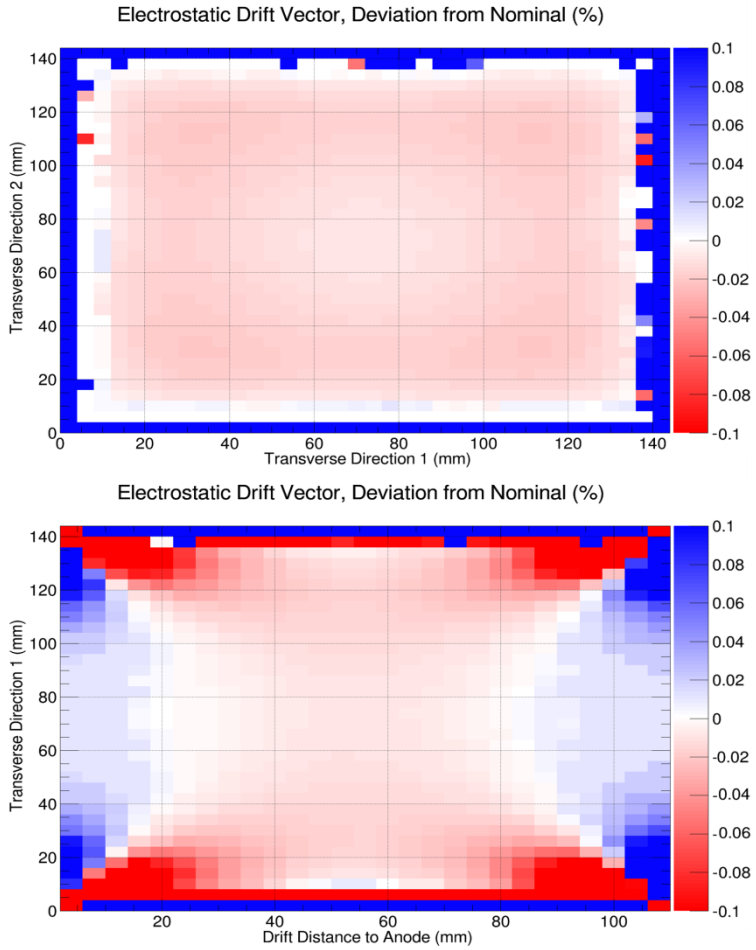

Figure 5 Deviation of the electric field vector from its nominal value along the drift direction. Upper: As a function of transverse position at the center of the fiducial volume. Lower: As a function of one transverse coordinate and the position along the drift direction.

The actual field cage foils have now been fabricated and delivered. Figure 6 shows the three sided kapton foil field cage mounted in its final assembly along with the high voltage electrode at the top of the drift gap. All of the kapton foils have been tested and were measured to have low leakage currents (< 1 nA) and were able to withhold a voltage difference of 400 volts between strips (corresponding to an overall drift field of 1 kV/cm).

The chevron readout board has also been fabricated and received and is shown in Figure 7. The board consists of 512 2x10 mm^2 chevron pads for which the signals pass through the board and are read out on the bottom of the detector.

Considerable progress was made on the overall mechanical design and the 3D model of the detector is now nearly complete. This included the final integration of the readout board (which is a separate detachable assembly along with the TPC GEM detectors), incorporation of the photosensitive GEM detector assembly (which is mounted on a movable stage that is remotely controllable from outside the detector), final design of the baseplate that supports all subcomponent assemblies, and the design of the overall gas tight enclosure (which includes the high voltage feed though for the TPC and optical ports for the laser that will be used to produce a source of localized ionization inside the drift region). Figure 8 shows some of the various components of the design.

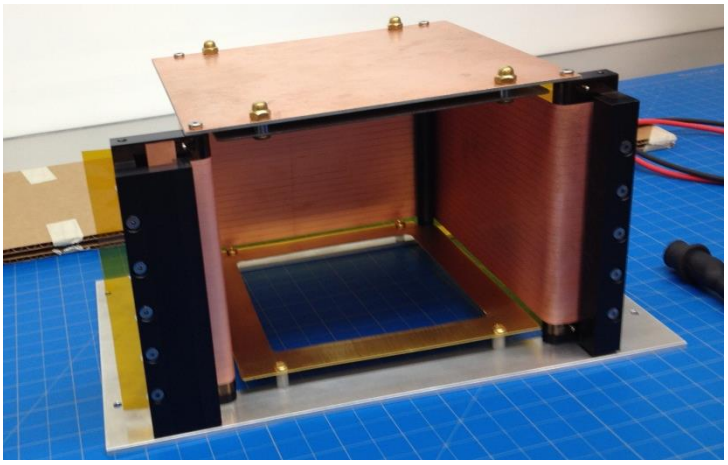

Figure 6 Three sided kapton foil field cage mounted in its final assembly with high voltage electrode on top.

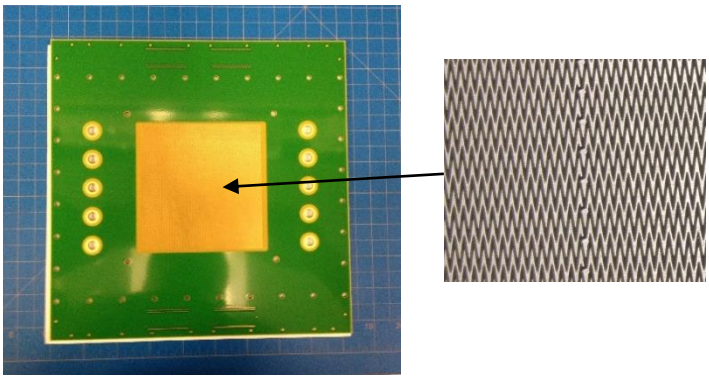

Figure 7 Chevron pad readout board.

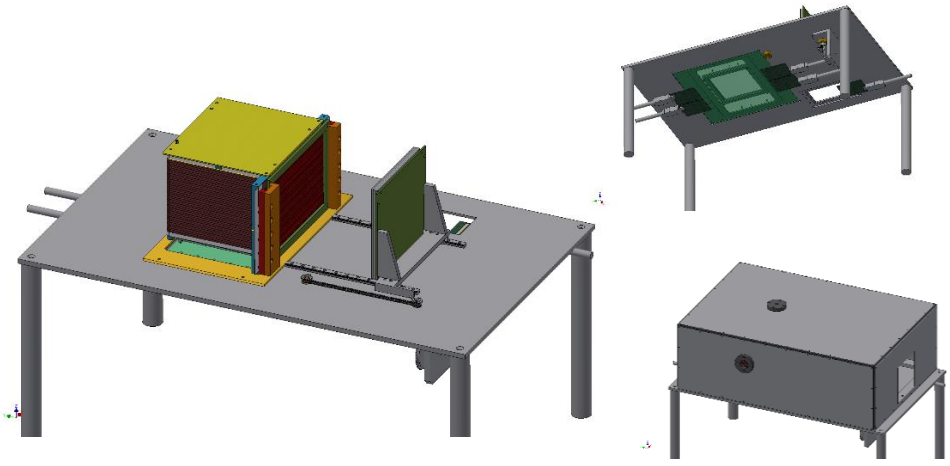

Figure 8 Mechanical design of the photosensitive GEM detector mounted on its movable stage to allow varying the distance to the TPC detector, underside of the baseplate showing GEM readout connections, and overall gas enclosure with ports for HV connection and optical windows for laser.

Measurements were also made on the properties of various gases that may be used with either the TPC alone or the combined TPC/Cherenkov detector. Figure 9 shows measurements of the drift velocities of a number of mixtures containing neon, which were studied mainly as gases that can provide low ion feedback (these gas mixtures are also being studied as potential gases for the upgraded ALICE TPC). Figure 10 shows the charge attachment measured in some of these mixtures over a drift distance of 32 cm.

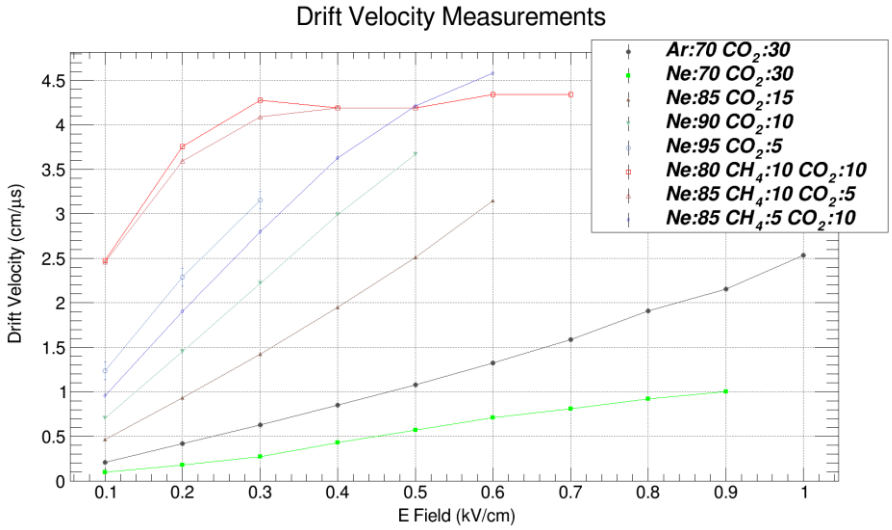

Figure 9 Drift velocity vs applied drift field for various gas mixtures containing neon.

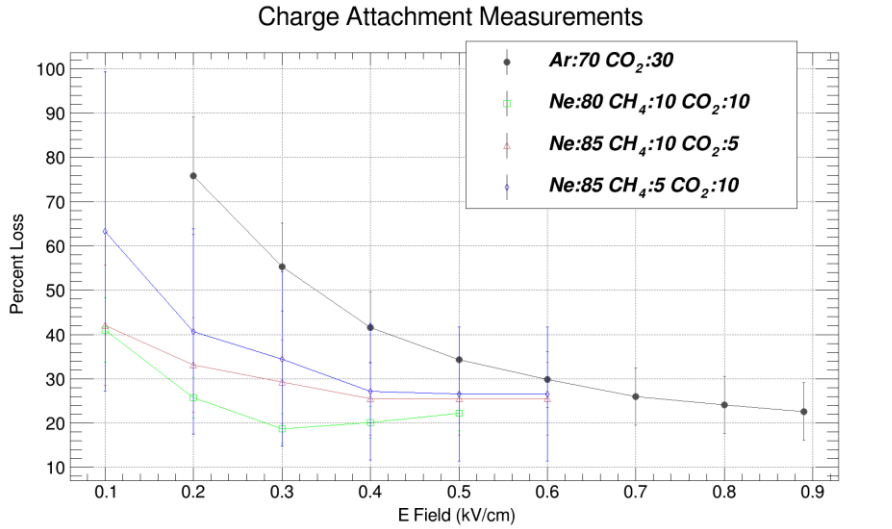

Figure 10 Charge attachment for a 32 cm drift distance for various gas mixtures containing neon.

Florida Tech:

Improved angular resolution for the 1-meter zigzag-strip GEM prototype

We successful devised an improved non-linear correction method using tracker information. For each cluster with a strip multiplicity N>1, we define a quantity $\eta \stackrel{\text{def}}{=} s_g - s_{max}$, where $s_g = \sum_{i=1}^{n} q_i \cdot s_i / \sum_{i=1}^{n} q_i$ is the centroid position of the cluster in terms

of strip number, s_i and q_i are strip number and charge (in ADC counts) for the i^{th} strip in the cluster, respectively; s_{max} is the strip number on which the maximum charge is collected in the cluster. This η quantity is a measure of the difference between centroid position and the maximum-charged strip. We separately correct for different cluster sizes because η has different characters for odd and even cluster sizes. Due to limits in statistics in the beam test data, we only correct cluster strip multiplicities N=2 and N=3 using corresponding quantities η_2 and η_3. Using tracks, exclusive residuals are then plotted vs. η and their profiles are fitted to appropriate functions. As shown in Figure 11, exclusive residuals are plotted vs. η_2 and η_3 and their profiles are fitted separately. A 10-degree polynomial for the η_2 case (Figure 11 (*left*)) is an approximate choice to get a better fit, while a serpentine function is used for the η_3 case (Figure 11 (*right*)).

By subtracting the η-dependent offsets obtained from the fit functions from the original residuals, we get significantly narrower overall residuals and hence improved resolutions. Figure 12 shows that the exclusive residual vs. η plot becomes much flatter after the subtraction. Inclusive residuals are corrected using the same fit functions. For the HV scan data, we combine data taken at different voltages to maximize the statistics for finding the best fit functions (we get similar results if we use only one run to make the correction, e.g. the run at 3250V). For the position scan data, each run has its own fit functions. Note that trackers do not need to be corrected since their resolutions are already good enough as they have straight strips with smaller pitch and consequently very small non-linear responses.

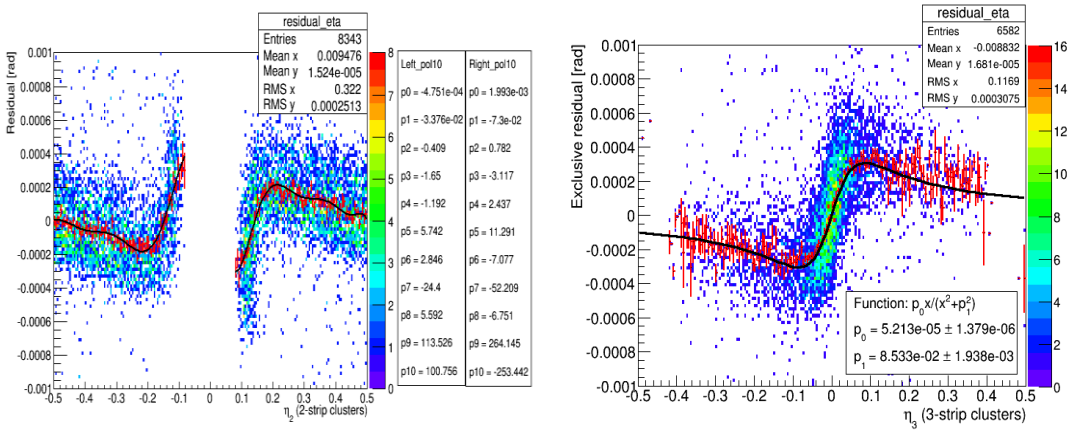

Figure 11 Exclusive residual vs. η_2 fitted with a 10-degree polynomial (left); exclusive residual vs. η_3 fitted with a serpentine function (right).

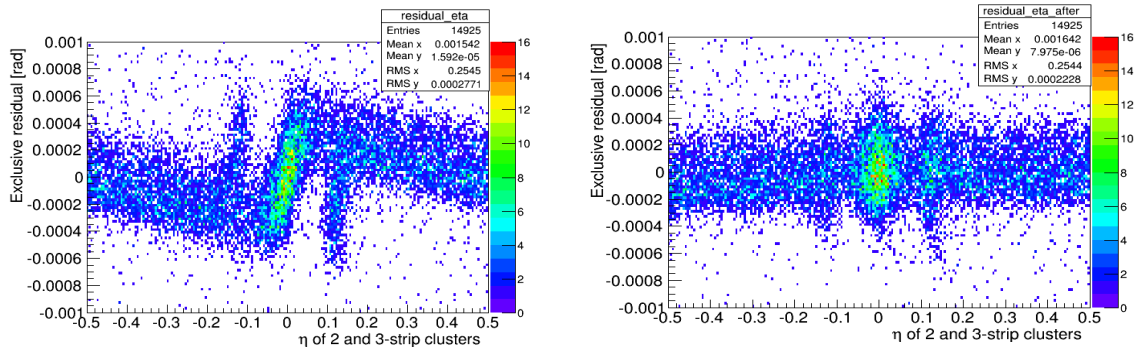

Figure 12 Exclusive residual vs. η for N=2 and N=3 clusters before (left) and after (right) correction.

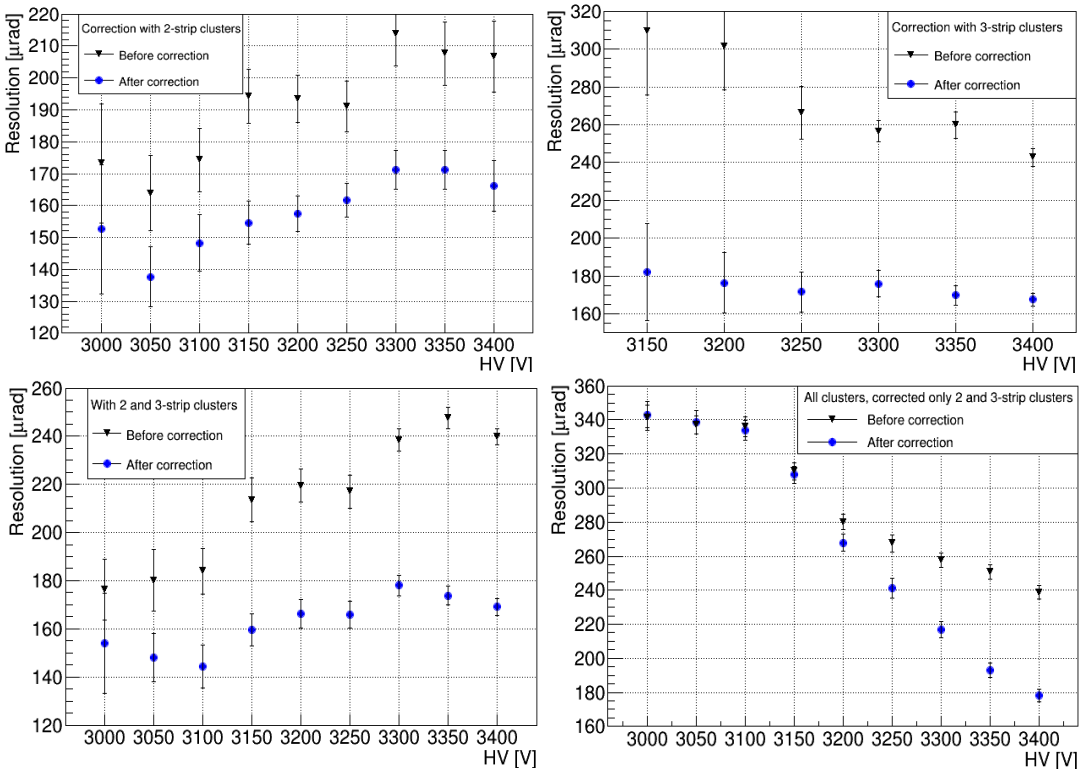

Figure 13 Angular resolutions at different voltages applied to the drift electrode in middle sector 5 of the zigzag GEM before (black) and after (blue) non-linear response corrections. Different plots are with different cuts on strip multiplicities of the clusters.

Angular resolutions after correction vs. HV in the middle of sector 5 on the zigzag GEM detector are shown in Figure 13 and compared with the resolution before correction. Different cuts on strip multiplicities are also compared. From the plots, we observe that resolutions are significantly improved for all HV points. For N=2 clusters the improvement is 12-20%, while for N=3 clusters it is about 30%. On the efficiency plateau, we get a resolution of around 170 μrad (corresponding to 12% of strip pitch) after correction.

Figure 14 shows resolutions before and after corrections at different positions on the zigzag GEM at 3200V. Here all strip multiplicities of clusters are used but only N=2 and N=3 clusters are corrected. It is evident that the resolutions are consistently improved in each sector. The improvement is about 8% for middle-sector positions, while it is smaller for the upper-sector positions. The improvement is smaller because now single-strip clusters are included that cannot be corrected because for these hits the centroid is identical to the strip center.

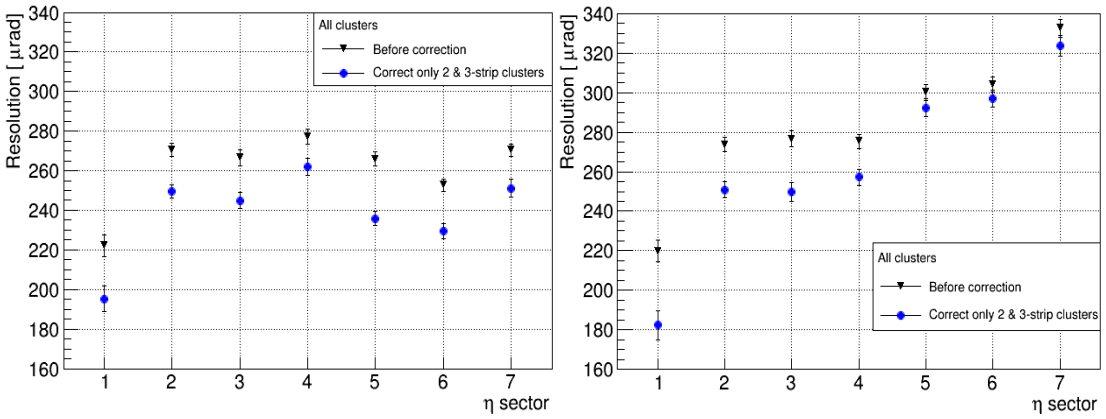

Figure 14 Angular resolutions at different positions for all strip multiplicities before and after corrections for drift electrode HV of 3200V. Left (right) plot is for positions in the middle (upper) of each sector.

These results were presented as a poster at the IEEE Nuclear Science Symposium & Medical Imaging Conference held in Seattle, WA in Nov. 2014. A paper for publication in NIM has been drafted on these beam test results. It is currently under internal review in our group.

Simulation of tracking in FNAL beam test setup (with A. Kiselev)

Alexander Kiselev recently applied the EicRoot software framework to the EIC forward tracking R&D effort. The motivation is to simulate the environment of the RD6 FLYSUB beam test at FNAL to get a more precise estimate of the effects of multiple Coulomb scattering when extracting detector resolutions from the track residual plots. The FLYSUB GEM tracker setup was ~3 m long and the overall material budget in the acceptance was relatively large. We estimate the total radiation length to be about 14% radiation length (Table 1), for which we naively expect an overall scattering rms width of 147 μrad for 32 GeV/c mixed hadrons and 39 μrad for 120 GeV/c protons using the standard mult. scattering eq. 32.15 in *Review of Particle Physics*. In our case, the data were taken with 32 GeV/c mixed hadron beams and we are getting a resolution around 170 μrad, which is comparable to the 147 μrad estimation, so this effect needs to be accounted for.

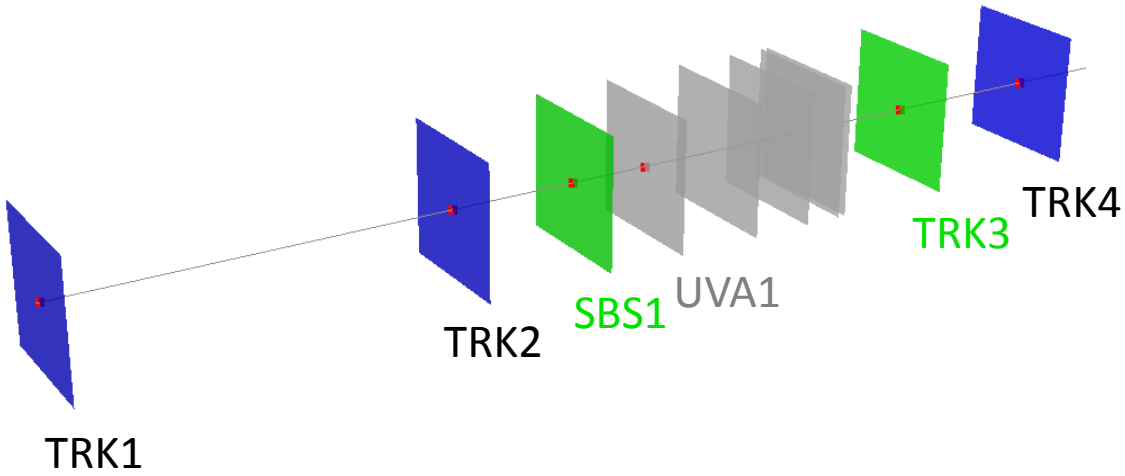

Figure 15 Simplified simulation setup for the RD6 FLYSUB beam test run at FNAL in fall 2013. The second grey rectangle from the left represents the 1-meter Fl. Tech zigzag EIC chamber. The other three grey chambers are small and medium-size zigzag detectors also built by Fl. Tech. See Table 1 for a complete list of detectors.

Table 1 Material budget in the Fermilab beam test configuration.

Detector	Gas gaps [mm]	Window mat./thick. [mm]	Readout mat./thick. [mm]	Rad. len. (%X_0)
Tracker 1	3/2/2/2	Mylar/~0.1	G10/kapton/honeycomb	0.32
Tracker 2	3/2/2/2	Mylar/~0.1	G10/kapton/honeycomb	0.32
SBS 1	3/2/2/2	Al+kapton	G10/kapton/honeycomb	0.345
UVA_EIC		Mylar/~0.1	G10/kapton/Rohacell foam	0.42
FIT_EIC	3/1/2/1	PCB/3.175	G10/3.175	3.88
FIT_30cm	3/2/2/2	PCB/3.175	G10/2.362	3.42
FIT_10cm_1	3/2/2/2	Mylar/~0.1	G10/2.362	1.5
FIT_10cm_2	3/2/2/2	Honey comb/3.175	G10/2.362	1.48
Tracker 3	3/2/2/2	Al+kapton	G10/kapton/honeycomb	0.345
Tracker 4	3/2/2/2	Mylar/~0.1	G10/kapton/honeycomb	0.32
Ar/CO2	88mm			~0.66
Air	~3m			~1
Total rad. L	14% X_0			

Alexander ported a custom tracking code based on a Kalman filter to EicRoot from HERMES sources some time ago; now he is applying it to this task. The basic setup shown in Figure 15 is used for the simulation. Tracking stations are simply represented as solid material blocks of appropriate thickness to represent the actual material budget (Table 1). The code works well with simulated tracks and confirms noticeable effects from multiple scattering at 32 GeV incident beam energy. With minor modifications and after appropriate tracker station alignment, the employed software framework also allows to import real data from the FLYSUB beam test to perform analysis of simulated and real data in exactly the same way. Using redundancy in reference tracker configuration and by disentangling the multiple scattering effects it was shown as a first step of this new analysis that indeed the Cartesian reference trackers have intrinsic resolutions of 50 - 100 microns.

The first outcome of this new study is that probed detectors have on average better spatial resolutions than anticipated before, and this conclusion is now based on quite solid tracking algorithms with a set of statistical analysis tools in hands. The software works with both parallel-strip and radial-strip GEM readouts.
It should be noted that the GEM module internal structure for physics simulations is represented in a much more detailed way than used for the FLYSUB resolution study. Materials in the acceptance (foils, gas gaps, readout plane) as well as the chamber frames are precisely described in the EicRoot geometry according to initial design drawings. The modular geometric setup in EicRoot allows to combine single GEMs of rectangular or trapezoidal shape in either a simple linear FLYSUB test beam arrangement or in complex structures such as the forward tracking disks of the eRHIC model detector (Figure 16). In all cases, sensitive volume mapping information is packed together with the ROOT TGeo geometry description, which allows to transparently use the same digitization and reconstruction algorithms if needed.

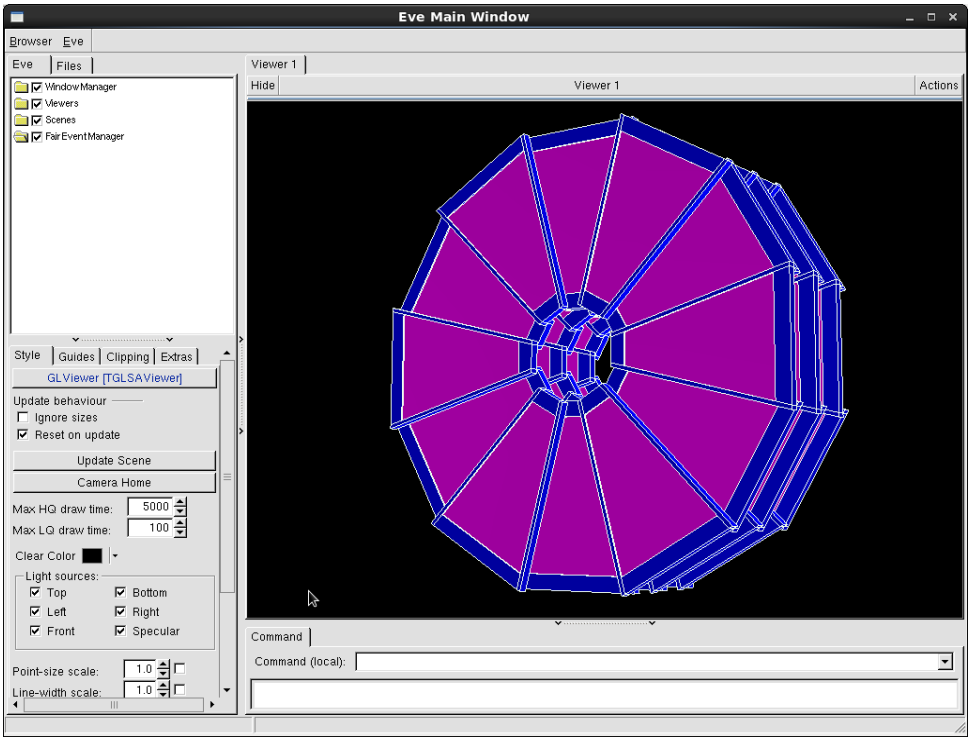

Figure 16 EICroot event display with three forward triple GEM disks of the eRHIC model detector tracker.

Design of next forward-tracker GEM prototype with domestic GEM foil

The Fl. Tech and U. Va. groups have been meeting biweekly with Bernd Surrow and Matt Posik (Temple U.) from the other EIC forward tracking RD group to discuss a common design of a "universal" large-area GEM foil and constructing GEM prototypes for EIC forward tracking (FT). The reason we need a universal GEM foil is that Fl. Tech is seeking to build the next EIC chamber prototype with a mechanical stretching method similar to the one that was used successfully for the first prototype (Figure 17) and tested in the FNAL beam, while the U. Virginia group focuses on building an EIC chamber with framed GEM layers where the GEM foils are glued to frames but the GEM layers are not glued together (see below). Both methods will keep the possibility to re-open the chamber and replace a layer in case of damage. The Temple group is currently contemplating yet another assembly procedure with permanently glued components.

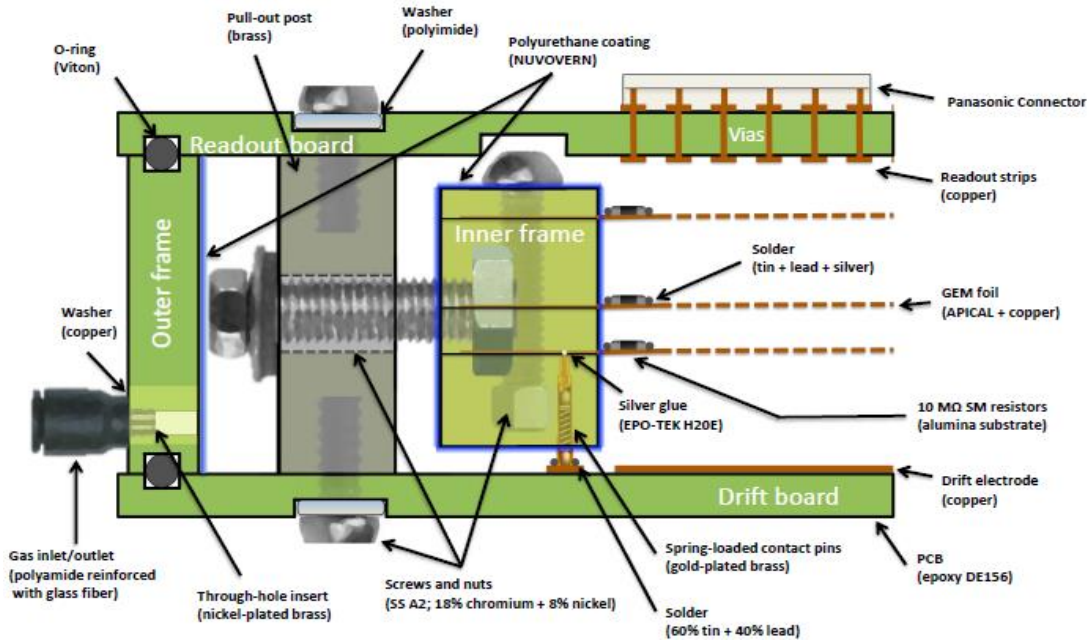

Figure 17 Diagram of large-area GEM chamber assembly with purely mechanical stretching method (from CMS GEM Upgrade Technical Design Report, under preparation).

Preliminarily, the joint FT group has agreed on a first common foil design, which has a trapezoidal shape with a 30-degree opening angle. The active foil area is ~95cm in length with an inner radius of 8 cm and an outer radius of 103 cm. Given that we are currently in an R&D stage, we have deliberately chosen an inner radius as small as possible that would bring the GEM as close to the beam pipe as possible. The motivation is to see with which assembly methods this is actually feasible for a 1m-long chamber. For a real EIC detector design, the inner radius could be increased as appropriate. The GEM foil comprises 26 HV sectors each with an area of ~110 cm^2. The 8 inner sectors are roughly azimuthal to avoid too much dead area at the inner radius while the outer 18 sectors are radial to facilitate easier connection of the sectors to HV at the outer radius. The frame width of an assembled GEM chamber will be about 1.5 cm. Figure 18 shows a mechanical design of this new foil design. A corresponding full disk for the EIC forward tracker built from such chambers is shown in Figure 19. In this design, the overlap between chambers is 3 cm with no dead area in the whole region.

Once we have finalized the design, we aim to have the first batch of these new foils manufactured by Tech-Etch, a US company that is planning to build large-area GEM foils domestically. The FT group has also been meeting on a biweekly schedule with TechEtch to monitor their progress on the production of GEM foils. They are now able to manufacture GEM foils of 50cm × 50cm size. For more information on the quality control of these new TechEtch foils, please see Bernd Surrow's RD report. Per our suggestion, TechEtch had a vendor's booth at the IEEE NSS/MIC conference to showcase their new GEM foils and to gauge market interest.

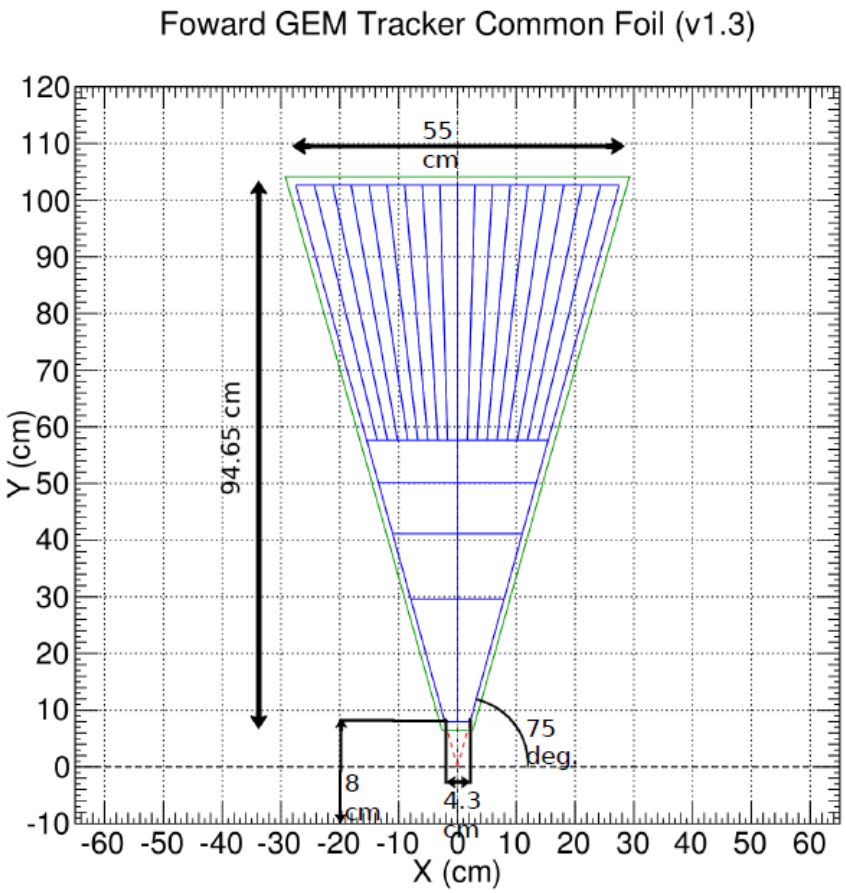

Figure 18 Geometry of the first version of a universal EIC forward tracking GEM foil designed by Florida Tech, U. Va., and Temple U. (courtesy M. Posik, Temple U.).

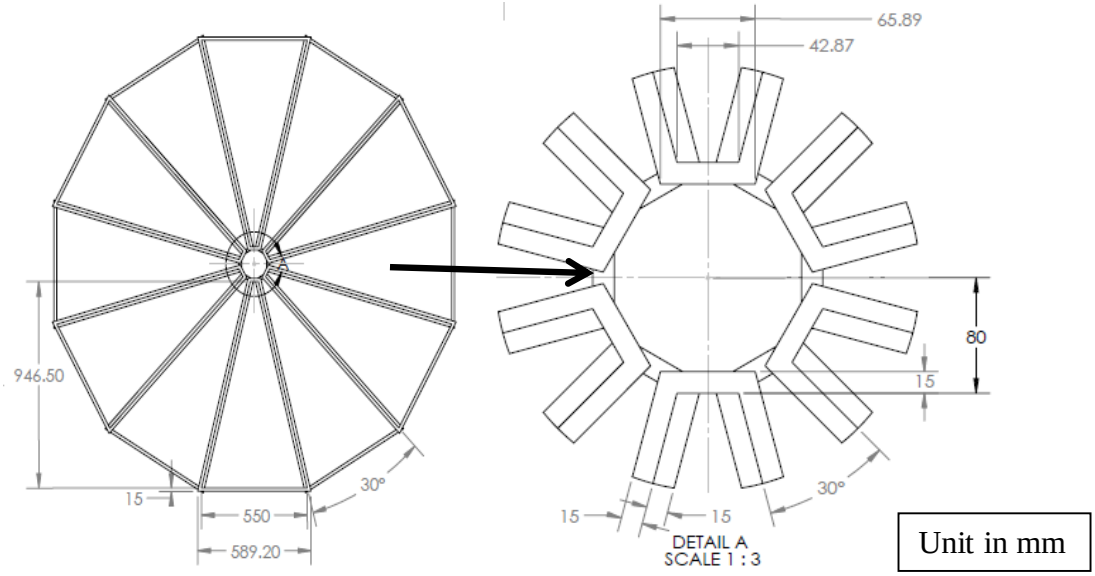

Figure 19 Design of EIC forward tracking disk assembled from 12 trapezoidal GEM chambers (left) of the type shown in Fig.6 and detailed view of the center region (R<15 cm). The foils of adjacent chambers are located right next to each other and the frames overlap for a total of 3 cm (right).

Finally, we have refurbished and tested a small electromagnet in the lab that produces a B field around 1 Tesla in an area of 8 cm × 8 cm × 2 cm (Figure 20). The measured field uniformity and stability in the center area of the magnet after turn-on are shown in Figure 21. We plan to use it to test the behavior of GEM chambers with zigzag readout in a magnetic field.

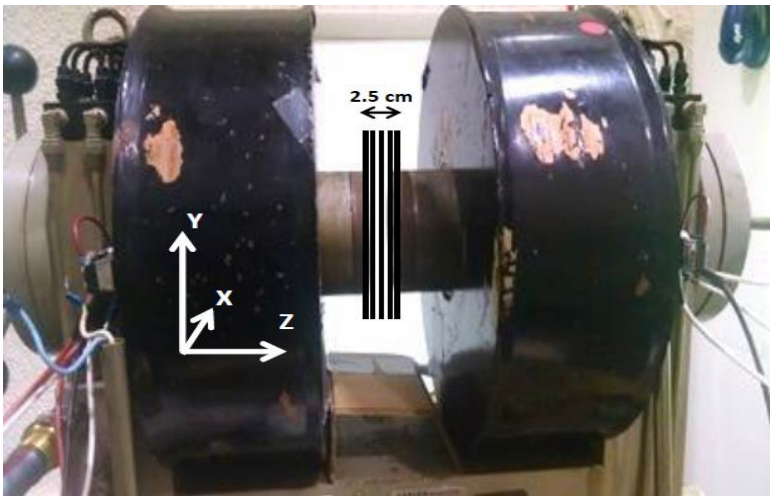

Figure 20 Small 1T electromagnet in Fl. Tech lab. The area in between the pole caps, where the B field is most uniform, is approximately 8cm × 8cm × 2cm.

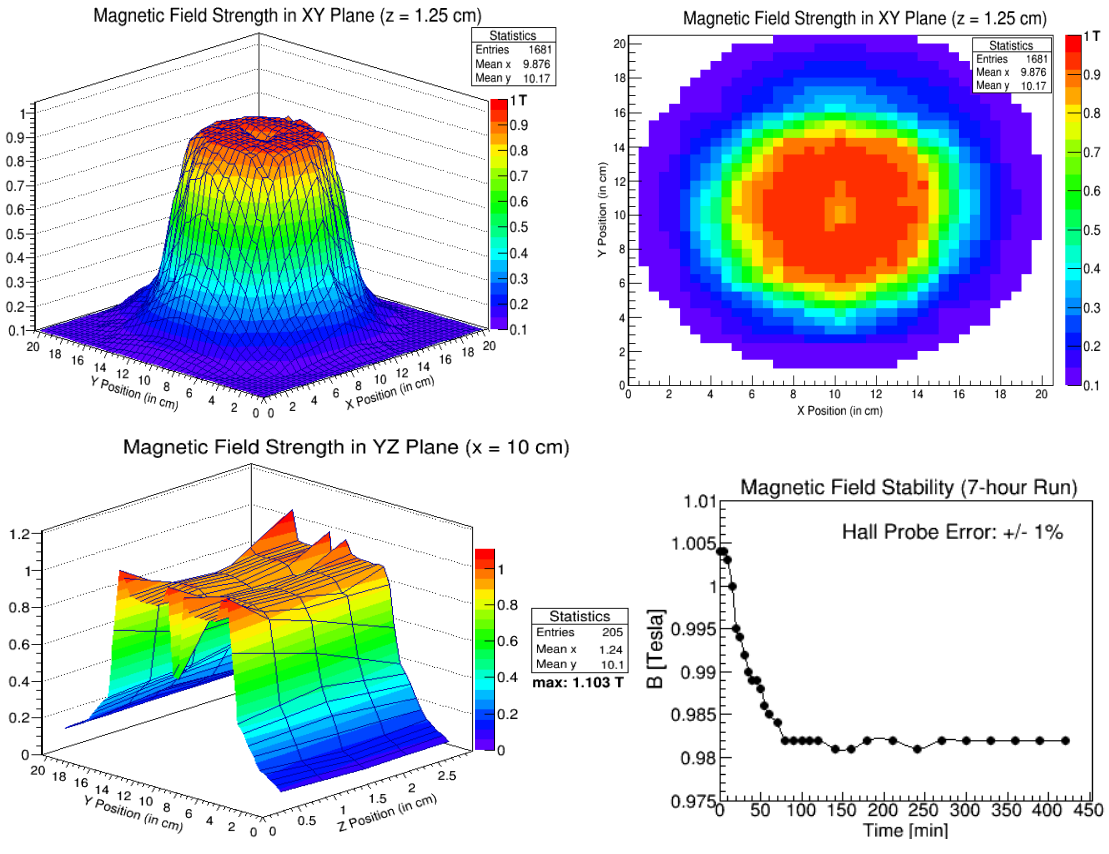

Figure 21 Magnetic field uniformity and stability in the center area of the pole caps.

Stony Brook University:

The description and results from the test-beam campaigns, SLAC and Fermilab FTBF were written in an IEEE journal (TNS) style and submitted to the editors. It is expected that the first round of peer-review will be finished by the end of January 2015. The results will be one of the first published experimental results from the various eRD groups within the EIC detector R&D efforts.
The following plots (Figure 22, Figure 23, Figure 24, and Figure 25) show the main results obtained and are the highlights of the publication. The upper panel of Figure 24 is a verification of the refractive index of CF_4 and is in agreement with published result: n_{CF4} = 1.00055. For the expected ring radius and width in the lower panel of Figure 24 several worst case scenarios were assumed: dispersion in the gas,

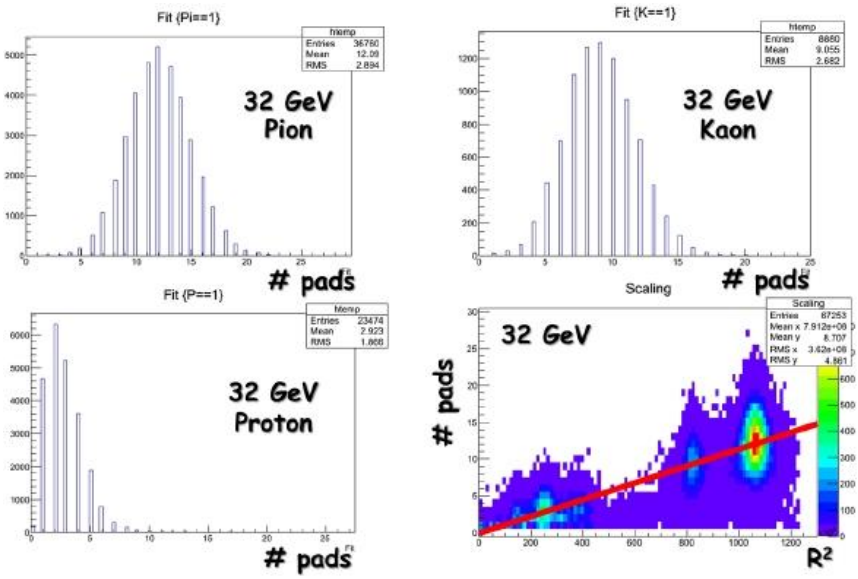

Figure 22 Distribution for the number of responding pads for various particles at the highest tested momentum at FTBF. The lower right picture shows the linear dependence of the number of pads on the squared radius.

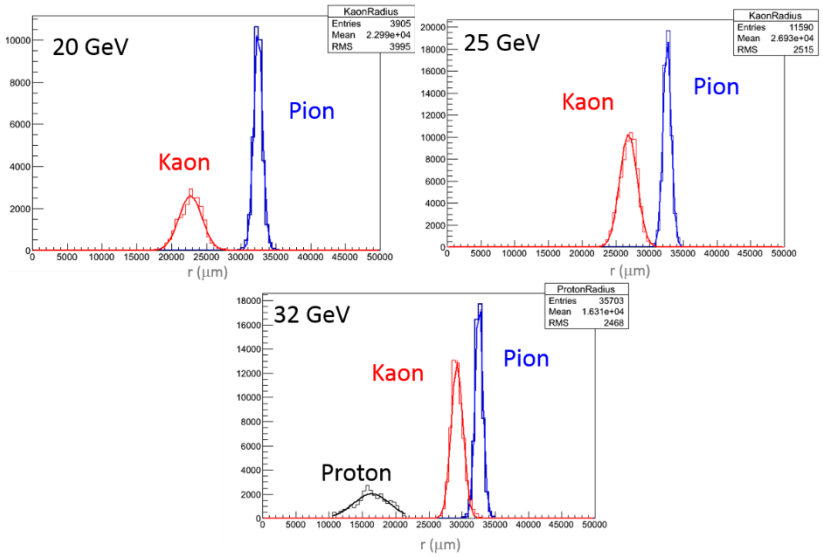

Figure 23 Particle ID with the RICH prototype. Clearly visible is the separation of the various particle species at same momenta.

segmentation of the RICH readout, momentum spread $\delta p/p$ = 5% of the FNAL beam line, and a constant term of 240 μm to account for all other factors.

A simulation framework was set up in order to simulate the dispersion of a charge cloud resulting from an electron avalanche in a multiple GEM stack. The origin of the charge cloud is of no concern and the procedure can generally be applied to any charge avalanche production with properly described parameters.
The simulation model is based on the "Telegraph-equation" which describes in one dimension the space-time evolution of a charge density on a wire. The model is extended to a plane by means of a two-dimensional RC network. Approximations

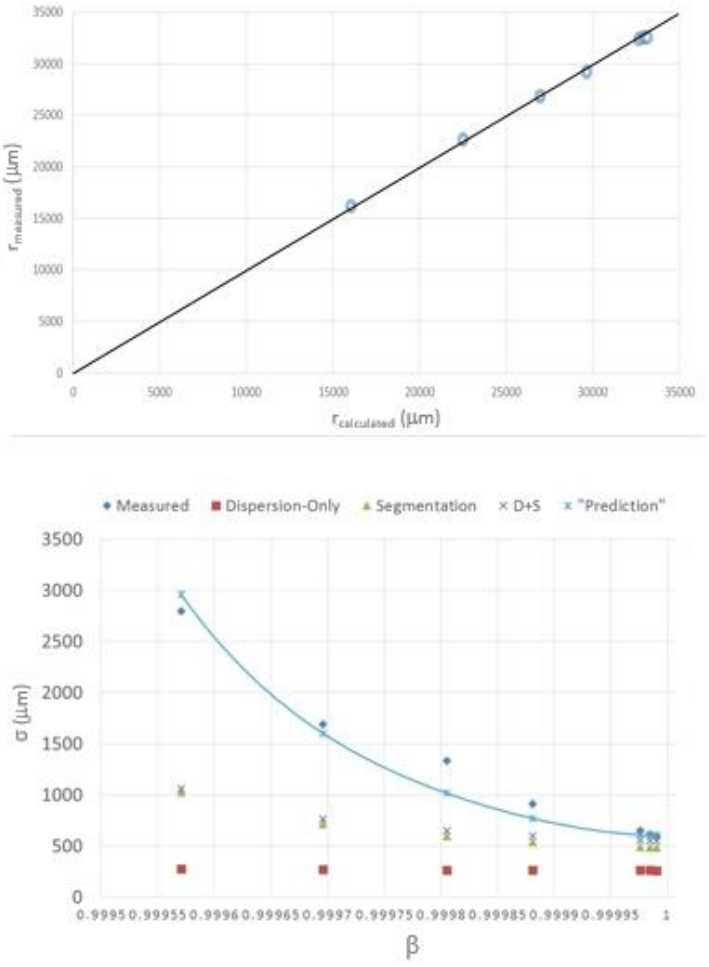

Figure 24 Upper: Expected ring radius compared to measured radius. Lower: Expected width accounting for various phenomena (see text).

are taken into account for obtaining a closed form of the solution to the Telegraph-equation by assuming a point charge (delta-function) deposited on the resistive surface with its edges at infinity. The delta-function is convoluted with a Gaussian for describing a finite charge distribution. This procedure describes the space-time evolution, i.e., dispersion of a charge cloud on a resistive anode, *Q(t)* and subsequently *capacitively or direct* coupling to a separate conductive pad readout. The geometry of the pads, in terms of size and shape is a major part of this investigation. Figure 26, right shows the dispersion of a charge signal (here: 8000 e^-) integrated over a rectangular pad with dimensions of 2x6 mm^2.
The simulation is also taking into account that the charge is not deposited instantaneously but rather has a space-time evolution itself while created: *R(t)* depicts the development of a charge cluster arriving on an anode and *L(t)* longitudinal distribution of that cluster. Also electronics shaping time effects, *A(t)*

are taken into account, i.e., the rise time of a signal and the decay in the electronic processing. All these effects need to be included as convolutions into the model. In Figure 26, left panel the individual contributions are shown, and in the right panel the convolution of the detector effects can be seen for a typical GEM setup. All responses there are shown for clarity in arbitrary units.
As a further step the simulation will be used to investigate the proper response of the pads to the signal with a pad response function. Single clusters with different widths will be created and varied in position across the pad. From this a theoretical pad response function is generated as a function of cluster position with respect to the pad center.

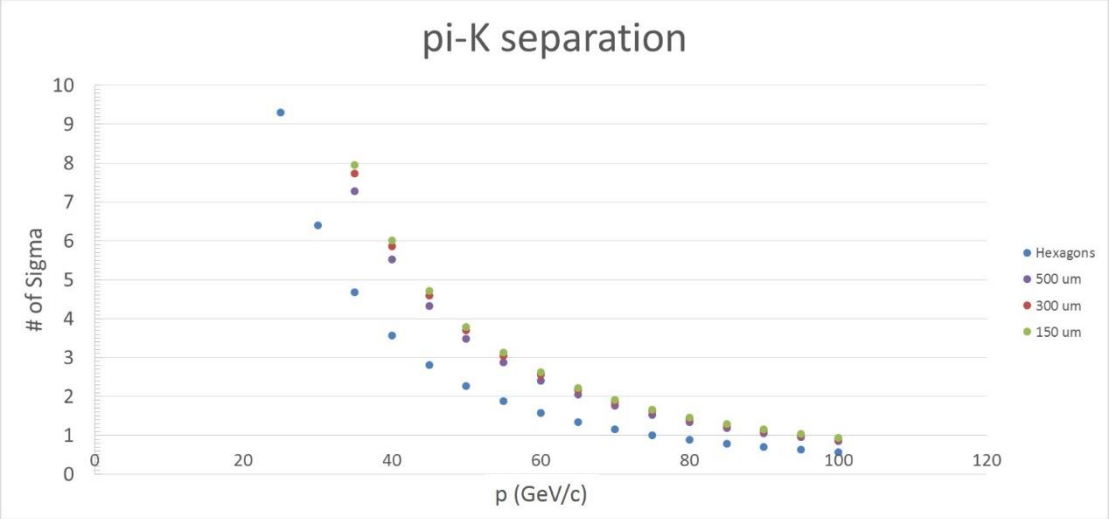

Figure 25 Pion and Kaon separation power.

The simulation is being evaluated and by varying the readout pads as well as parameters of the resistive anode a set of optimized readout schemes will be developed and produced to be tested within laboratory conditions.

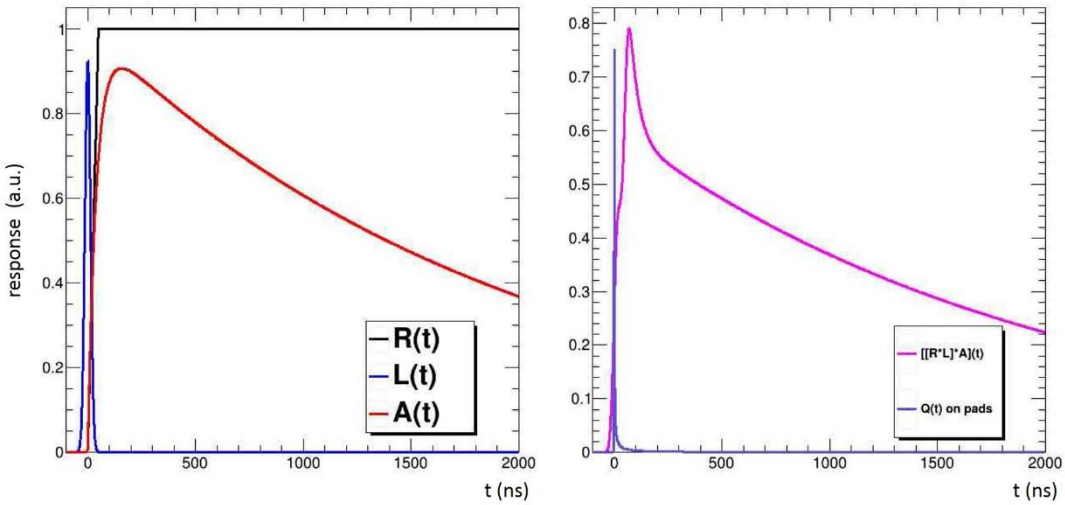

Figure 26 Contributions of various detector effects to the charge diffusion on a resistive anode (see text).

University of Virginia:

Spatial resolution studies of EIC-GEM prototype

We reported in the June 2014 progress report, the preliminary results of data analysis of the Fermilab Test Beam Facility (FTBF) run performed in October 2013 at FNAL with the EIC-GEM prototype. The GEM detectors arrangement for common UVa and FIT setup during the FTBF test beam is shown in Figure 27.
We have continued the data analysis effort with a main focus on improving position resolution performances of the detector with fine tuning the alignment parameters of both the EIC-GEM prototype and the GEM detectors used for the tracking on the MT6 setup at the FTBF.

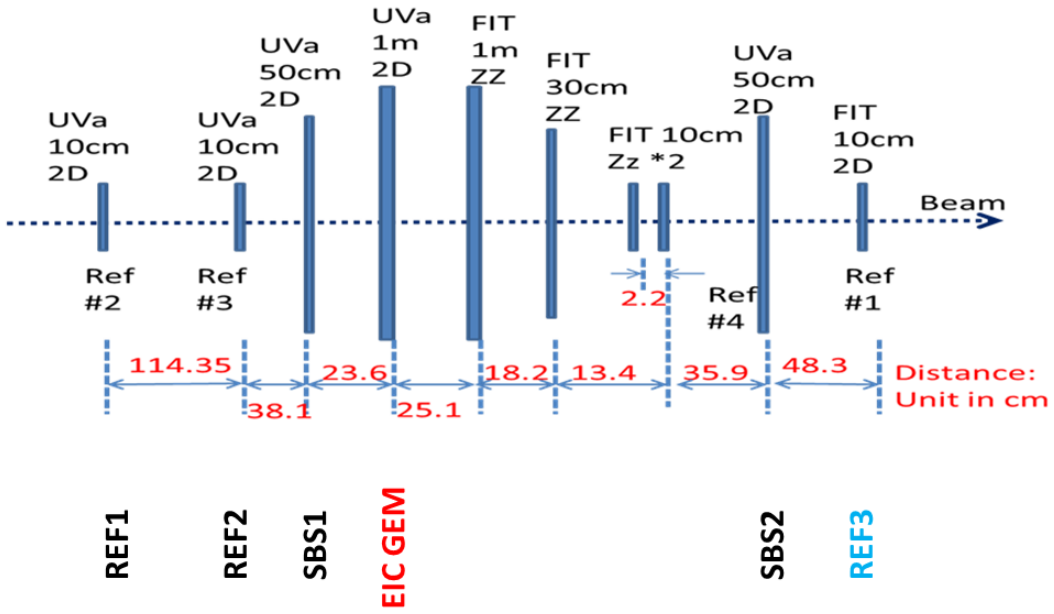

Figure 27: Common GEM detectors setup on MT6b stand at FTBF by UVa and FIT

The alignment involves the correction of the offset in x and y direction and the rotation in the x-y plane perpendicular to the direction of the beam for all the detectors. We study the impact of this correction on the spatial resolution of the

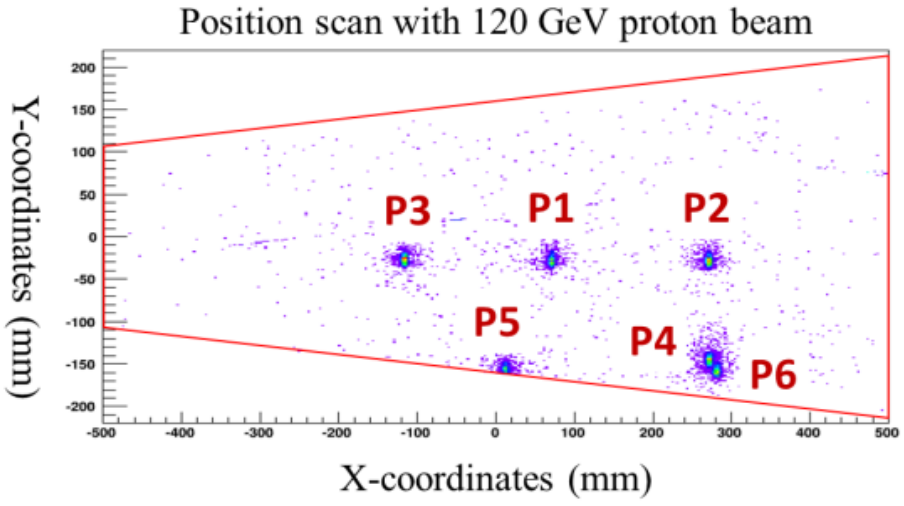

Figure 28 2D distribution of 120 GeV proton beam reconstructed from the six positions scan at FTBF.

EIC prototype. The alignment involves fine tuning of the corrections of the relative offset in x and y direction and the rotation angle in the x-y plane with respect to the first tracker REF1 (see Figure 27) of all the other detectors. We study the impact of these corrections on the spatial resolution of the EIC prototype at different locations on the chamber using data from the proton beam position scans run (see Figure 28) during FTBF campaign.

Correction of the beam position offset in x and y for all trackers.

The correction of the offsets in x and y for is done in two steps: The first step is a coarse correction using the proton beam position from each chamber. Then in a second step, we produce new offset parameters for each run by computing the shift of the beam position in x and y for each detector relative to tracker REF1 which is the most upstream to the beam.

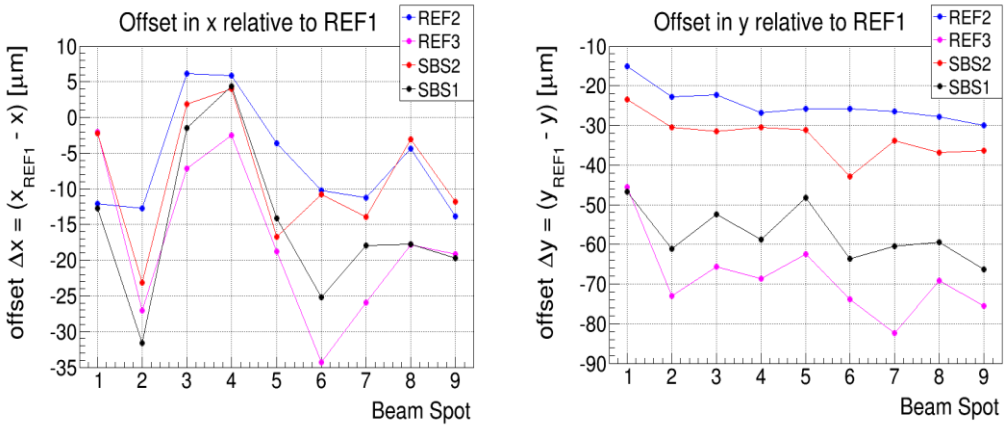

Figure 29: Beam position offset in x (left) and y (right) relative to REF1 for all other GEM detectors

Figure 29 shows the relative offset in x and y for the small GEM chamber REF1 and REF2 as well as for larger GEM prototypes SBS1 and SBS2. We observe a relative shift of up to 40 μm in both x and y of the beam position for some runs. The shift is on average bigger for detectors further downstream from tracker REF1. The shift is also more pronounced in x direction and could be explained by the fluctuation in the direction of the incoming beam provided by the facility.

Correction of the relative rotation of the trackers

We also studied the misalignment of the detectors relative to tracker REF1 in term of the rotation of the (x, y) plane perpendicular to the beam direction. The rotation angles are computed after the offset correction described in the previous paragraph. Figure 30 shows the rotation angle for two trackers REF2 and REF3 relative to REF1 for the six beam position scan runs before and after the offset correction in x and y is applied. There is a significant variation (up to 14 mrad for REF3) of the rotation angle from one run to the other when the offset correction is not applied. The variation of the rotation angle is less than 2 mrad for all detectors after the (x, y) offset correction.

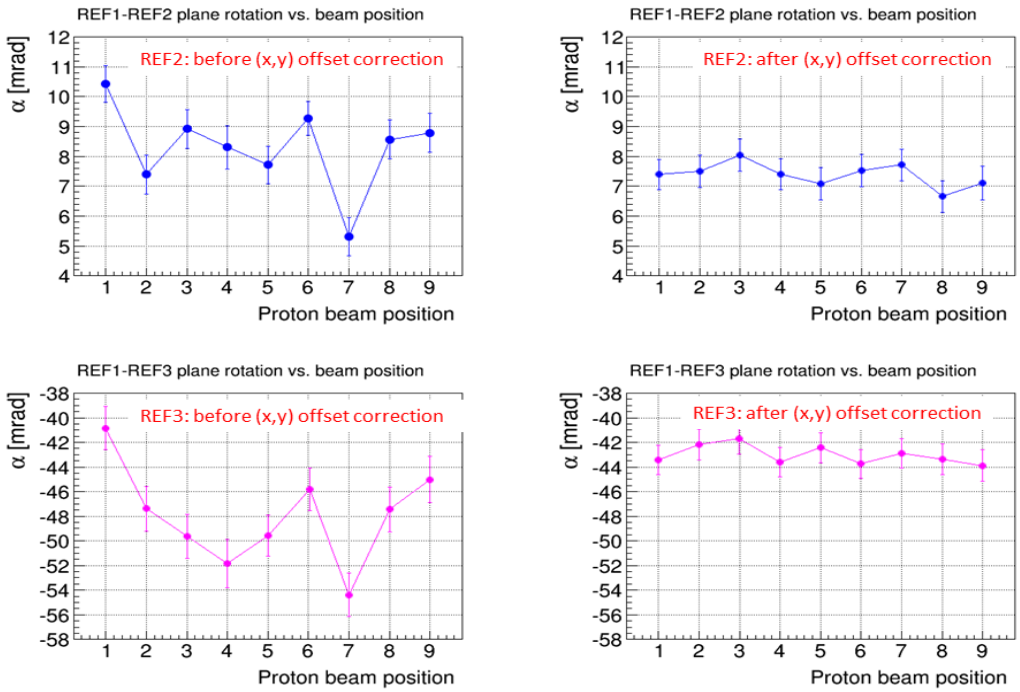

Figure 30: Rotation angle relative to REF1 for trackers REF2 and REF3 for different beam position before (left) and after (right) offset correction in x and y

Effect of the correction on the track fit residuals

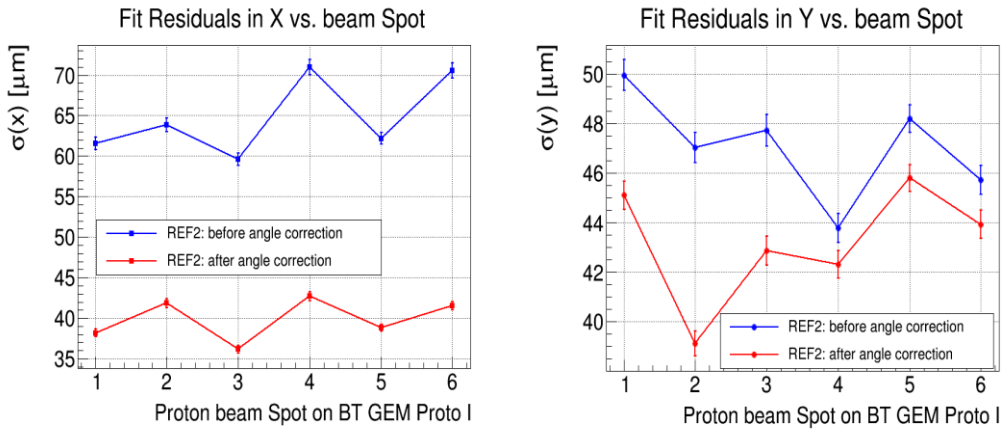

Figure 31: Track fit residuals in x (left) and y (right) for tracker REF3 before (blue) and after (red) offset and plane rotation corrections

Figure 31 shows significant improvement of the track fit residuals in (x and y) for tracker REF3 after the position offset and rotation angle corrections. Similar improvement of the residuals is observed for all the trackers. The residuals are obtained using the inclusive method in which data from REF3 are also used for the track fit. This explained the width of the residual as low as 35 μm for REF3 in x for a detector with expected resolution around 50 μm.

Effect of the correction on the resolution of EIC prototype

The effect of the fine alignment corrections on the resolution performances of the EIC GEM prototype is shown on Figure 32.

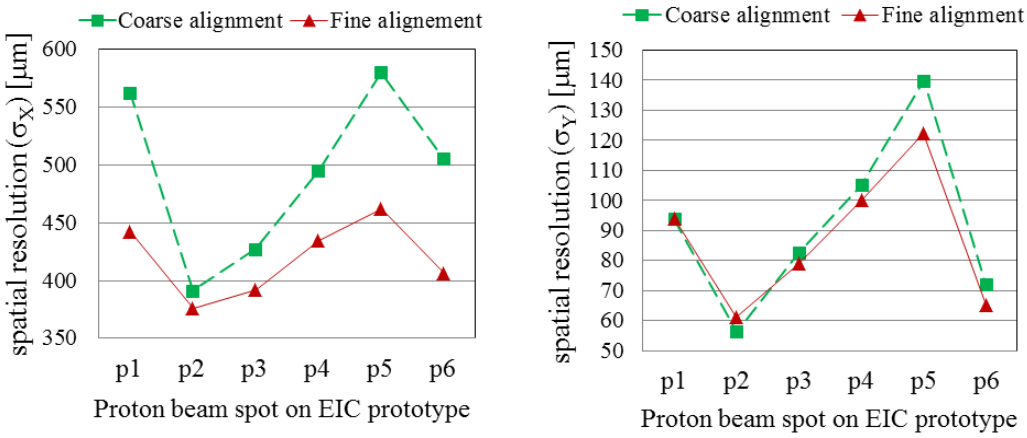

Figure 32: Impact of alignment corrections on the resolution in x (left) and y (right) for EIC-GEM.

On the plots of Figure 32, the "coarse alignment" refers to the results on resolution performances that were reported in the June 2014 progress report. The "fine alignment" refers to the current results with a fine tuning of the offset and rotation angle corrections for each position scan run. The improvement after the corrections is clear for both x and y coordinates. The resolution improved by as much as 20% for some of the position scan runs in the x-direction. The difference is less pronounced for the y-coordinates but still clearly established.

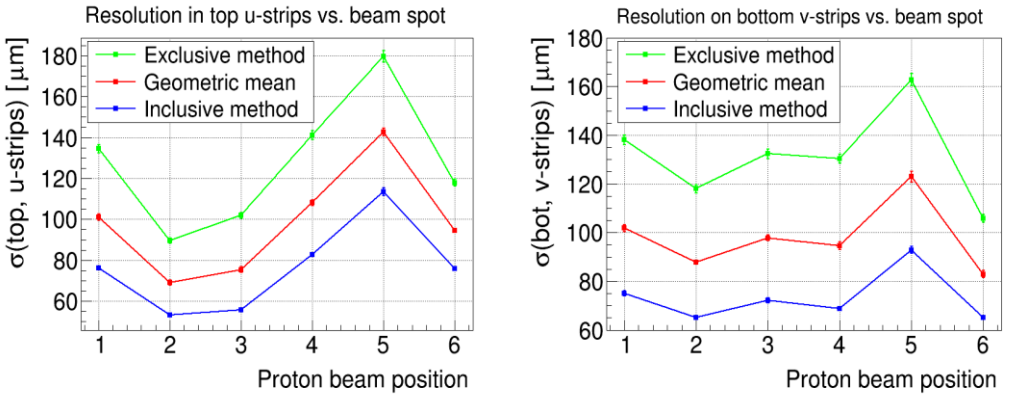

Figure 33: Residuals for top and bottom strips of the EIC GEM u/v readout board at different beam spot position obtained respectively from exclusive (green) and inclusive method (blue). The data in red is the geometric mean of the exclusive and inclusive and define the resolution.

The resolution varies between 370 µm and 460 µm in x and between 60 µm and 120 µm for y. Figure 33 shows the residuals using exclusive and inclusive method and the resolution measured for the u-strips (top layer) and v-strips (bottom layer) of the readout. In order to obtain the residual independently for top and bottom strips, the expected x-coordinates, x_{Fit}, from the track fit is used. The resolution is lower than 100 µm for almost all different beam positions and for both u and v strips. The overall non uniform resolution from one location to the other can be explained by the different length of the u and v strips at different location in the

chamber. The peak at P5 observed for all the results is due to the beam at this location, hitting the edge of the detector resulting to a truncated strip clusters.

Effect of track fit error and Multiple Coulomb Scattering.

We estimate the impact of the detectors configuration, used to obtain the track fit, on the EIC GEM resolution when one uses the geometric mean from inclusive method and exclusive method to calculate the resolution. To do so, we performed the fit using two set of tracking detectors and compute the exclusive, inclusive resolution and the geometric mean for each run. In the first configuration, the fit is performed using a set of three GEM trackers REF1, REF2 and SBS1, all located upstream on the FTBF setup, in front of the EIC GEM prototype (see Figure 27). These detectors were all built with relatively low mass and therefore we expect a small effect of the scattering in the track fit. In the second configuration, tracking detector REF3 is added to the previous three detectors for fit. As one can see on the setup in Figure 27, tracker REF3 is the further away downstream to the beam with five additional GEM chambers in the way of the proton beam between EIC GEM prototype and tracker REF3. Four of these five detectors are from Florida Tech chambers with considerably more material due to different construction technique used for their assembly. Using the first tracking detector configuration with all 3 low mass detectors upstream would yield a better result in evaluating the resolution of the EIC-GEM chamber, because the effect of multiple scattering could be neglected compared to the second configuration with additional REF3 placed far downstream.
However, when using the geometric mean to calculate the resolution, having all the tracking detectors on one side of the probed detector (EIC-GEM) leads to a systematic underestimation of the calculated resolution compared to the real position resolution when the expected resolution of the probed detector is significantly higher than the resolution of the tracking detectors. With the second configuration where REF3 is also used for the fit and is located behind the probed detector (EIC-GEM), the impact of the systematic error from the geometric mean method is greatly reduced.

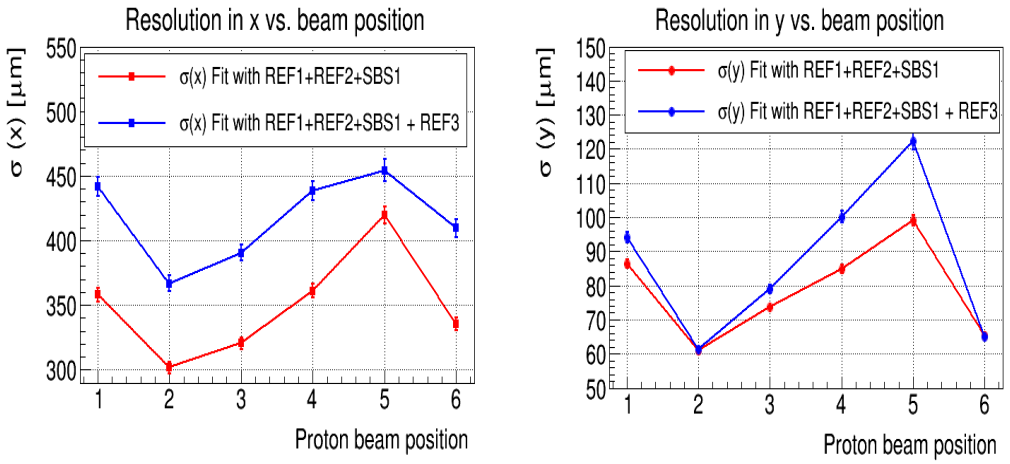

Figure 34: Impact of track fit error and multiple scattering on the resolution in x (left) and y (right) using two tracking detectors configuration for the fit.

Figure 34 shows the resolutions in x and y of the EIC GEM for the two tracking detector configurations. The position resolution calculated from the geometric mean is in seemingly better for both x and y coordinates when only the three trackers upstream are used for the fit. A 20% improvement of the resolution is seen for all runs (beam spot) for x-coordinates and varied from 5% to 20% for y-coordinates. The apparent improvement of the resolution when using data from 3

trackers configuration for the fit can be explained by concurrent effect of the expected improved resolution from the negligible contribution of multiple scattering and the negative impact of the artefact error created by the geometric mean method. This artefact effect could easily be corrected by deriving the appropriate correction parameters from a dedicated Monte Carlo simulation of the test beam setup provided that the resolution of the tracking detectors is known. We plan in the near future to pursue the resolution analysis in this direction.

Angular resolution of EIC-GEM prototype

Figure 35 shows the resolution of the EIC-GEM prototype in cylindrical coordinates. The average resolution σ (r) in the azimuthal direction is about 350 μm with a peak reaching 420 μm at the location P5 as expected and the radial direction, the average angular resolution σ(φ) is 50 μrad with a peak reaching 70 μrad at P5.

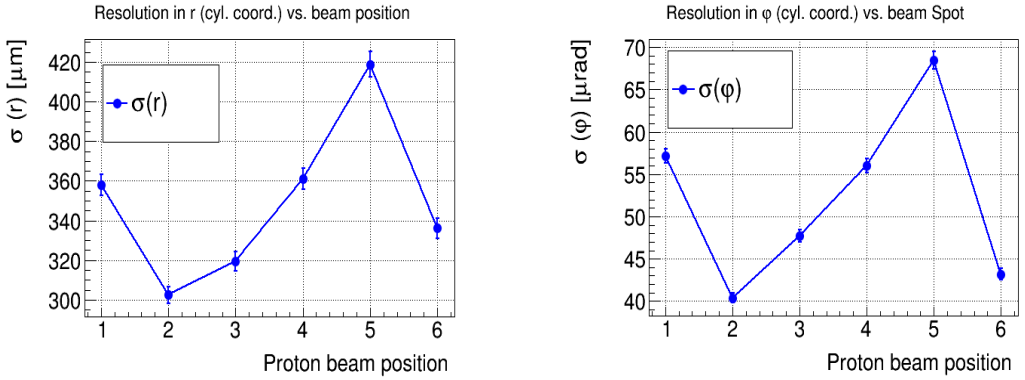

Figure 35: resolution σ(r) of the EIC GEM in the azimuthal direction and σ(φ) for various beam positions

Update on the R&D effort on the improved design, assembly and performance of the EIC-specific GEM prototype.

Light-weight and low-mass detector.

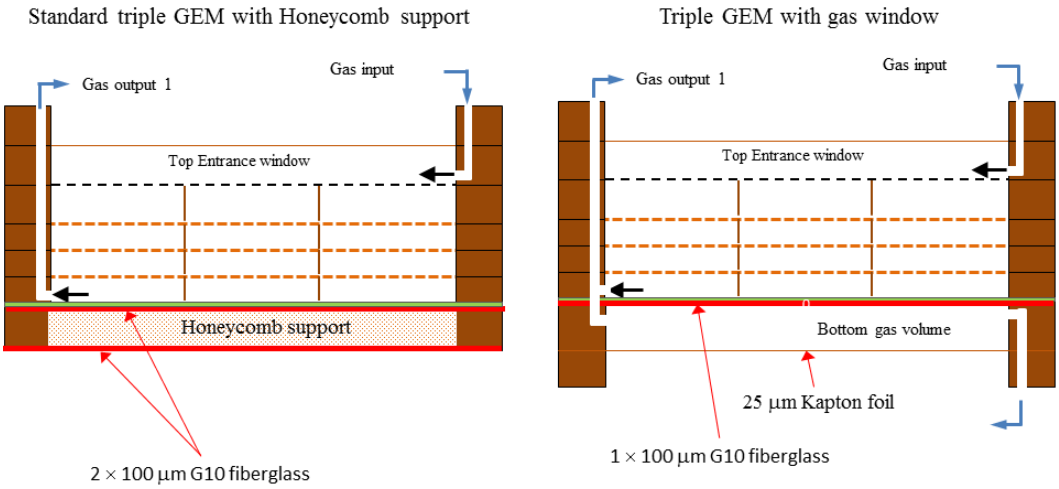

Figure 36: Removing the bottom honey comb support of standard GEM to reduce material

The COMPASS-like 2D flexible readout board in a standard Triple-GEM detector is typically glued to a mechanical support based on a 3 mm thick Nomex honeycomb sandwiched between two sheets of 100 μm fiberglass G10 material. A way to reduce even further the material amount of these detectors is to replace the honeycomb

support by a gas volume with 25 μm Kapton foil as window as illustrated on the right plot of Figure 36.

We are in building the first **"honeycomb-less"** GEM prototype as a proof of concept using spared GEM foils and readout boards. We have already received from CERN one 2D SBS GEM readout board glued onto 100 μm fiberglass G10 skin and we expect to build and test the chamber early 2015.
Another idea under investigation is the replacement of conventional GEM foil by **"Copper-less"** GEM in which the foil completely stripped off of the 5 μm copper electrode on both sides which account for a total of 30 μm copper material (10 μm per GEM foil with 3 GEM foil per detector) removed from the detector per GEM foil. The electrical contact is provided by the residual extra thin chrome layer between the polyimide (Kapton) and the copper layer. We recently acquired three small size (10×10 cm^2) "Copper-less" GEM foils from CERN and we are building a small triple-GEM chamber. We plan to test the prototype in our new x-ray test box to study the ageing and discharge capability at high ray. This if successful will constitute a major breakthrough toward low mass light GEM detectors

New assembly technique:

In the standard assembly technique of triple GEM that we refer to as "closed geometry" in this report, the different layers of the triple-GEM detector (GEM foils, drift cathode foil and readout board) are stretched and glued to their respective support frames and the frames are in turn glued together in the final detector assembly. In this case, once the chamber is assembled, it is impossible to replace faulty GEM foils if needed.

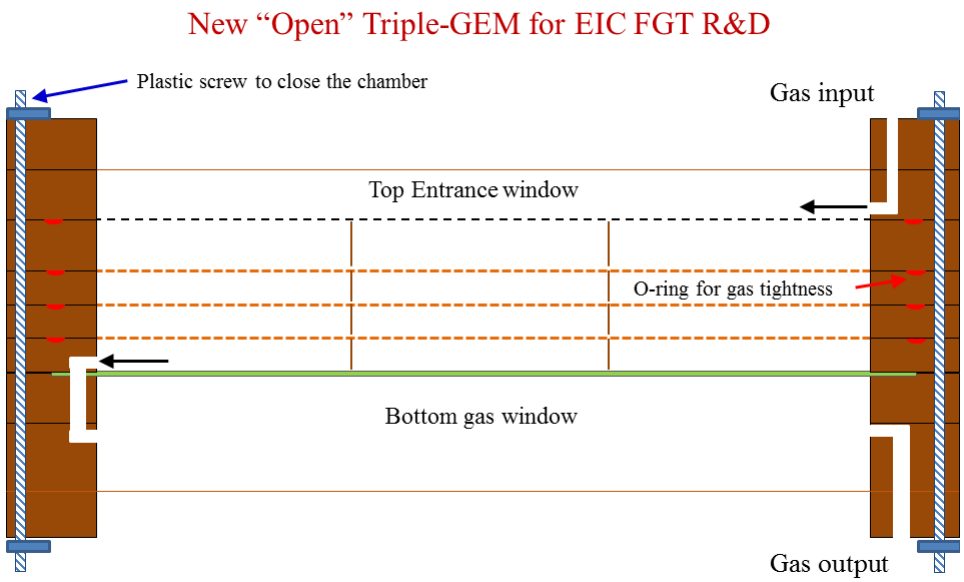

Figure 37: Sketch of the new assembly technique: GEM support frames are not glued together but held tight with plastic screw and O-ring to seal the chamber against gas leak.

We propose a new technique for the assembly of GEM detectors, described in the sketch of Figure 37 with the GEM foils still on to their frame, but the frames are no longer glued in the assembled chamber but stacked together and held with plastic screws with O-ring between the frames to ensure gas tightness. We are currently testing the idea on a large area (120×55 cm^2) GEM chamber (see Figure 38) that we are in charge of building for new proton radius experiment (pRad) in Hall B at JLab scheduled to run in the Fall 2015. We plan to apply the lesson learned from the pRad GEM to the EIC-GEM in the first half of 2015.

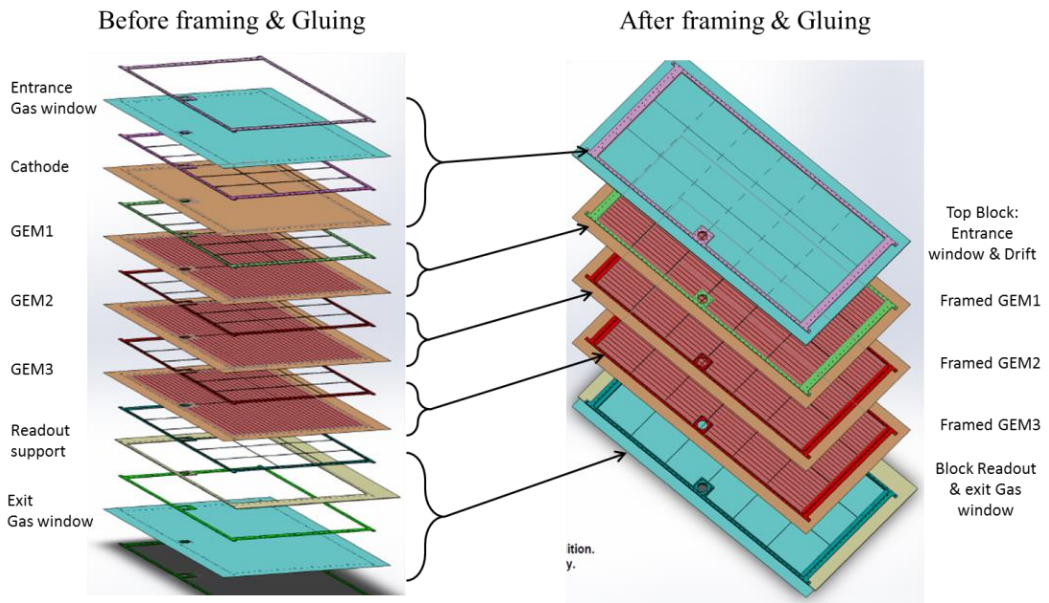

Figure 38: 3D exploded view of the parts of the triple GEM where the framed foils are not glued together based on the pRad GEM chamber design.

Yale University:

3-Coordinate GEM

Careful electrical measurements of the 600 μm pitch 3-coordinate readout boards and visual scanning has shown many areas where the copper between readout elements was not completely etched. This results in shorts between the readout elements. Since the pads are connected together to functionally form strips even a single short between two pads from different coordinates shorts two full "strips" together. Thus a modest number of shorts can make the board unusable. It was known from previous work on fine pitch 2-coordinate readout that the 600 μm boards are at the limit of what can be reliably fabricated. It appears that indeed the yield for 600 μm pitch 3-coordinate boards is unacceptably low, especially if the technique is scaled to much larger boards than the 10 cm × 10 cm boards used for these tests. For the 800 μm data, modest progress on the analysis was made. The final analysis and publication remain to be completed.

Hybrid Gain Structure for TPC readout – 2 GEM plus Micromegas

At the start of this period we had just received a borrowed MMG with a 400 mm pitch strip readout. During the period we designed and purchased 4 other readout plane designs, built 2-GEM+MMG chambers with these and embarked on an extensive program to characterize the performance of these chambers under a variety of conditions. Figure 39 shows a typical configuration for these studies. Tests were done with 10 cm x 10 cm active area.

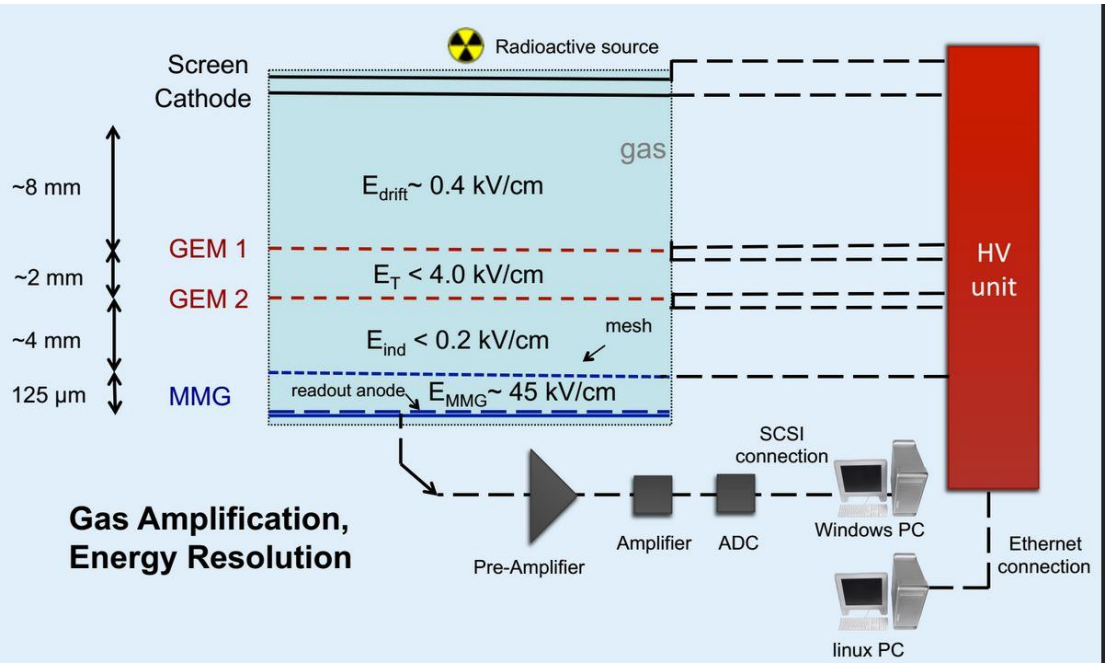

Figure 39. Typical setup for measuring gain and energy resolution for a 2-GEM+MMG hybrid gain structure.

Very early in optimizing the voltage settings to achieve good energy resolution and low IBF the following principles became clear:

- Higher gain for the top GEM (GEM 1) gives better energy resolution. This is not unexpected as the same behavior is observed for any multiple element gain structure. The "statistics" should be dominated by the original ionization so the first gain element should have a gain of at least a few.
- Higher gain in the top GEM results in higher IBF. Again, this is not unexpected since there are no elements "above" the top GEM to capture back flowing ions.
- Higher transfer field between the two GEM's (E_T) reduces IBF.
- Lower field between GEM 2 and the MMG mesh reduces IBF. The IBF from the MMG is proportional to the ratio of the field above the mesh to the field below the mesh.

Using these principles as a guide scans of operating voltages were made. Gain and energy resolution are measured with a ^{55}Fe x-ray source. The energy resolution is characterized as the width (std. dev.) of the resulting peak in the pulse height spectrum divided by the peak position. Figure 40 shows a typical spectrum. As illustrated it is possible to resolve peaks from X-ray ionization produced above the top GEM, between the 2 GEM's and between the bottom GEM and the MMG. This allows us to measure the relative gain of each element in the gain structure. We note that the compromise between good energy resolution and low IBF leads to running the GEM's at rather low gain: Top GEM effective gain ~ 6x and Bottom GEM < 1x. In this mode the bottom GEM serves more as a screen to catch back flowing ions from the MMG. This is why the "MMG only" peak in the spectrum is at higher pulse height than the "MMG+bottom" GEM peak.

Ion back flow is measured in the same conditions with small changes in the instrumentation as shown in Figure 41. A more intense source is used and DVM's

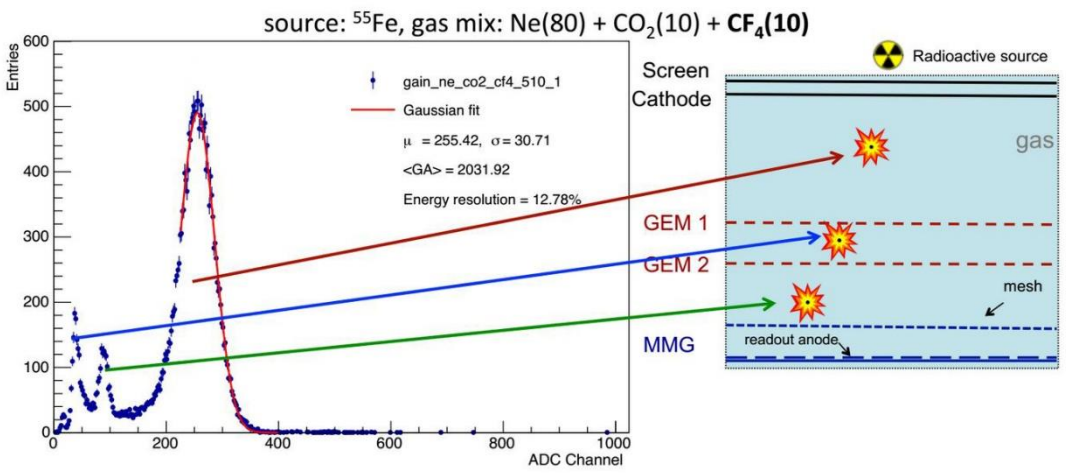

Figure 40. Typical pulse Height spectrum from ^{55}Fe source. The different peaks represent ionization created in different regions as illustrated.

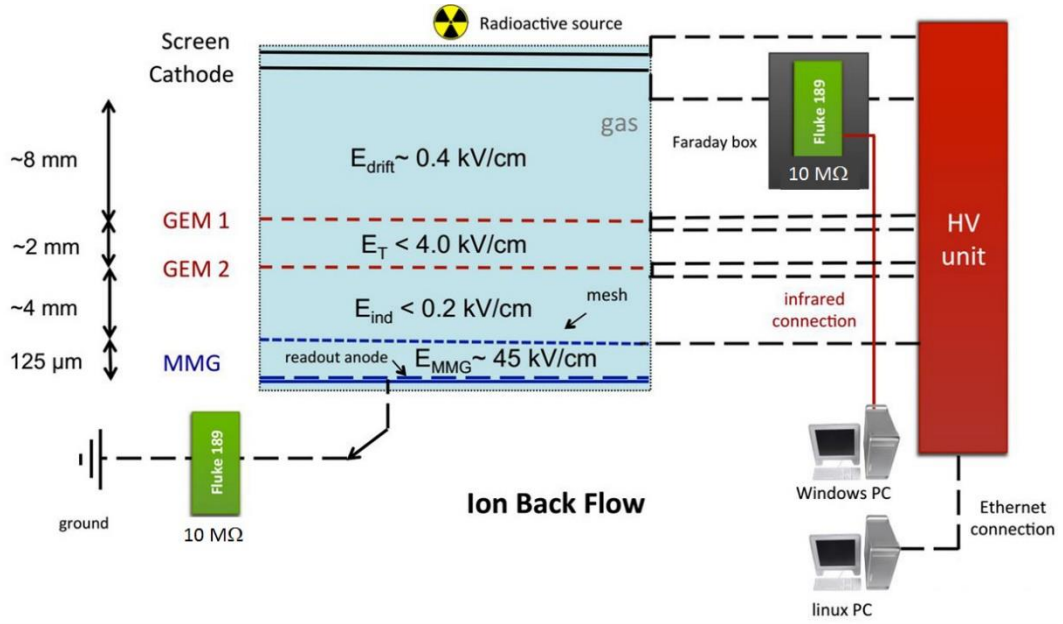

Figure 41. Setup for measuring ion backflow. The meters are used with mV setting (least count = 1 mV) to measure the voltage drop across the 10 MW internal resistance. The battery powered meters can be floated to high voltage and read out via an IR to USB connection to a computer.

are used to measure the anode and cathode currents. The "screen" electrode in the sketch in Figure 41 prevents ions produced in gas outside the chamber from being collected on the cathode and giving a spurious ion current. The meter measuring the cathode current is floating at the cathode voltage and to achieve maximum sensitivity is shielded from pick up noise in a metal box. Typically measurements are made with anode currents of ~100 nA resulting in cathode currents of > 100 pA. Table 2 shows results for a typical scan of operating parameters. In this case the MMG mesh voltage is varied (hence MMG gain) while adjusting the two GEM voltages to keep the total gain approximately the same. IBF as low as 0.3% can be achieved with energy resolution less than 12% for chamber gains in the range 2000 – 2500. This result is typical of many scans of voltages, fields and working gas.

Table 2 Table 3. Energy resolution (column 5) and IBF (column 7) for 2-GEM+MMG chamber. MMG mesh voltage is scanned (1st column) while GEM voltages (3rd, 4th columns) are changed to keep the overall gain ~2000 – 2500. Operating gas is Ne + 10% CO_2. Transfer field (between GEMS) = 3kV/cm, induction field (between bottom (midl) GEM and MMG mesh) = 0.875 kV/cm.

V, MMG	<G.A.> MMG	dV1 (top)	dV2 (midl)	σ/Mean, % Fe55	<G.A.> All	IBF, %
380	650	220	210	11.25	2500	0.45
385		215	205	11.3	2260	0.41
390		210	200	11.3	2040	0.4
395		210	200	11.6	2270	0.34
400	810	210	200	11.8	2530	0.31

We also investigated chamber performance with different gas mixes. Figure 42 shows a comparison of mixes with CH_4 (more quenching) and CF_4 (fast electron drift). For the CF_4 mix, the transfer field (between the two GEM's) is limited due to loss of gain at high fields. This is likely due to capture of electrons by CF_4. Increasing the transfer field from 1.5 kV/cm to 4 kV/cm results in a reduction of effective chamber gain by about 10x. These measurements were performed at chamber gains of 4000 – 4500 with higher MMG gain so the IBF is generally lower than the data in Table 2. These data indicate that for good energy resolution and lower IBF mixes with CH_4 are preferred.

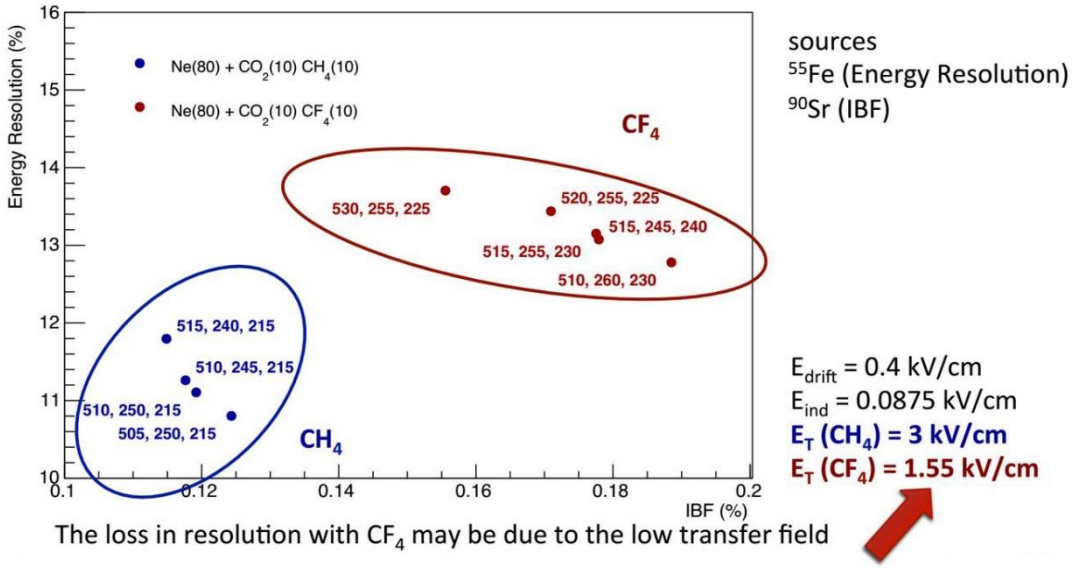

Figure 42. Comparison of energy resolution *vs.* IBF for two different gas mixes. The numbers near the points are: MMG mesh voltage, top GEM voltage, bottom GEM voltage respectively.

The robustness of the 2-GEM+MMG chamber against discharges was studied by incorporating an 8 cm ionization volume above the gain structure with a ^{241}Am source (6 MeV α) at the cathode to provide large ionization. The results at several different MMG and chamber gains are shown in Table 3. It is not simple to translate these numbers to operation at a collider however the results are encouraging.

Table 3 Discharges measured at several different gains. The chamber gas for this test is Ne+10%CO2 and the bottom GEM voltage is 210 V.

	MMG, V	dV, GEM top, V	<GA>, MMG	<GA> (x e3)	Statistics	Number of sparks (MMG)	Number of sparks (GEM)
Test to 10^8 α at various MMG gains, chamber gain kept at ~2000 by varying top GEM gain	460	230	500	1.9	1.06 e8	0	0
	475	225	656	2.05	1.15 e8	0	0
	485	220	838	2.15	1.2 e8	0	0
Low statistics tests – increase MMG gain and chamber gain to see onset of sparks	490	220	926	2.38	2.1 e5	0	0
	495	220	1044	2.68	1.5 e5	0	0
	500	220	1160	2.97	1.1 e5	0	0
	505	220	1315	3.37	5. e4	25	0

The influence of the readout plane geometry was also studied by observing the MMG mesh voltage at which sparking began (≥ 1 spark per 10 minutes with illumination by a moderate rate source) for different readout geometries. These measurements are shown in Table 4. The tests were done with 90%Ar, 10%CO_2 gas using a modest rate (~1 kHz) ^{55}Fe source. The "Strips" readout plane has 400 μm pitch strips with 100 μm gaps between strips. The "IROC" readout plane is similar to the ALICE inner chamber pad plane with 4 mm × 6.4 mm pad pitch, 100 μm gap between pads, 400 μm gap between pad rows and an 800 μm unfilled via in the center of each pad. The chevron pad plane has 6-chevron pads with 4 mm × 6.4 mm pitch, 100 μm gap between pads, 400 μm space between pad rows and small filled vias.

Table 4 Spark threshold measurements for 3 readout plane geometries.

Type of MMG	Sparking: Vmesh, <GA>	E-resolution (σ/Mean)
IROC	530 V, ~1600	10.5%
Strips	570 V, ~2200	9.5%
Chevron pads	555 V, ~2150	15.%

From the table and from further studies on simpler geometry (4 pads, 5 cm x 5 cm with 100 μm gaps, no vias) and electrostatic calculations and gain simulations it is evident that since the readout plane is one electrode of the MMG the best performance in terms of energy resolution and sparking threshold is achieved by using readout plane geometry with small filled vias and the smallest practical gaps between readout elements.

What was not achieved, why not, and what will be done to correct?

Brookhaven National Lab:

The final design was not fully completed due mainly to lack of designer time. The drawings are being done by a single designer who works for the PHENIX group and his time available to us is very limited. The main item remaining is to detail the base plate, which should take several additional hours. We expect to have this completed by early January, at which time, the base plate and all of the other remaining mechanical components can be fabricated.

We will use the CERN SRS readout system for our initial studies with the TPC, but due to limitations in its buffer depth (< 1 μsec), this will limit the range of the drift volume that we will be able to read out. We also have several other systems, including several Struck SIS 3300/3301 modules that can digitize 24 channels up to 10 μsec, and a set of CAEN V1742 digitizers that provide up to 5 Gsps sampling for up to 128 channels, which will allow us to study such things as timing and pulse shape in great detail. However, we are still searching for a more suitable readout system that will provide greater flexibility for the entire detector. We expect to receive the first readout cards that use the new VMM2 chip designed by the BNL Instrumentation Division early next year and we will certainly investigate these. We are also investigating the GET TPC electronics, which has been widely used by other groups for small to modest sized TPCs. Finally, we will be following the development of the SAMPA chip that is being developed to read out the upgraded ALICE TPC as a possible long term solution for the future.

We did not upgrade the optics of our VUV spectrometer due to lack of funding. However, we will soon need this system to be fully operational as we begin to study the photosensitive GEM part of TPC/Cherenkov detector.

Florida Tech:

The beam test results have not yet been submitted for publication because of the multiple Coulomb Scattering that affects the resolution studies with the FNAL beam test data by a significant factor due the large number of detectors and significant material in the beam. We expect that the final results on the resolution for the zigzag GEM detector will be lower than the above stated preliminary results.

Stony Brook University:

The development of the simulation framework was delayed due to unsuccessful recruiting process early in the semester as well as important participation in the upgrade efforts in the PHENIX experiment. We are now back on track and the investigations are ongoing.

University of Virginia:

We have yet to start working on the new u/v stereo angle 2D readout board for the EIC-GEM prototype with the front end electronics connectors on the outer radius of the GEM. As described in the previous section, the analysis of the data collected with the first EIC prototype during the FTBF test beam is still ongoing. A large amount of data was collected and the analysis with finely tune alignment and calibration parameters has taken longer than initially expected and delayed the work on the new readout design. In addition, for practical reason, the design of the readout board has to be done once we have a clear idea of the geometry of the common GEM foil and the constraints imposed the various requirements. We are planning to complete the readout design work by early 2015.

We also initially planned to study the possibility to implement the work done at BNL by Dr. Craig Woody's group on the mini-drift into the large area EIC-GEM with 2D u/v readout in order to ensure good spatial resolution at large incoming angle. This activity has been postponed for since a meaningful study requires to build have a suitable prototype. The ability to re-open the next prototype would give us the flexibility required in term for the mini drift capability study by playing with the drift region gap. We anticipate resuming this study once the prototype is built and initial characterization are performed.

Yale University:

3-Coordinate GEM
The analysis and publication was not completed in the past period. Further effort will be devoted to this in the coming period.

Hybrid Gain Structure for TPC readout – 2 GEM plus Micromegas
Planned investigation of different support methods for the MMG mesh and options for segmenting the MMG mesh were not done.
For typical TPC pad sizes, MMG fabrication experts advise that supporting the mesh only with ridges in the spaces between pad rows is not adequate. Given this it is better to regularize the pattern of support pillars to the pad pitch so the pattern of pillars is identical for every pad.
Segmenting the MMG mesh to reduce the energy in a discharge proves to be quite challenging. There are other methods to accomplish this goal that we will investigate in the coming period.

Future

What is planned for the next funding cycle and beyond? How, if at all, is this planning different from the original plan?

Brookhaven National Lab:

- Finish construction of the TPC/Cherenkov prototype detector
- Test the detector in the lab, starting first with the TPC detector alone using available electronics. Measure S/N ratio, verify drift field parameters, study different drift gases. Measure tracks with cosmic rays and develop software for track reconstruction.
- Install standard GEM detector in position of photosensitive GEM and carry out series of HV tests to establish optimal working position.
- Upgrade optics of VUV spectrometer.
- Construct photosensitive GEM detector. Measure QE of photocathode. Install photosensitive GEM in TPC detector.
- Test combined TPC/Cherenkov detector in the lab and measure with cosmic rays.
- Carry out beam test of combined TPC/Cherenkov detector.
- Acquire and test suitable readout electronics for the TPC portion of the detector. It would be highly desirable if this could be done prior to the beam test.
- Complete the analysis of the Minidrift GEM detector and publish the results

Florida Tech:

In the Fermilab beam test analysis, we need to figure out in detail how much the multiple scattering is affecting the resolutions for the zigzag GEM, so we will keep working on the beam test simulation together with Alexander Kiselev.
We expect to have the first common FT GEM foil design finalized by the three collaborating groups in January 2015 and presented to Tech-Etch and CERN for a technical review.
The Florida Tech group will need to design components for mechanical stretching of the new FT GEM foils and get them manufactured by US companies. We would prefer to source all EIC FT materials in the US, not only the GEM foils. The chamber material budget is an important issue that we have to consider carefully in the design. We plan to use low-mass materials in our design as much as possible.
As part of this new design effort, we will design a new version of our cost-efficient zigzag-strip readout board so that we can assemble an EIC tracking GEM prototype with this readout and test it.

Stony Brook University:

In the following, second part of FY2015 it is planned to finalize the study for the charge dispersion and to produce a set of feasible readout boards and investigating the improved position resolution in a test-beam setup, for instance at SLAC or FTBF again.
The results of this project will be in general interesting for the other groups in our consortium, if not for other groups within the EIC R&D projects.

University of Virginia:

For the next cycle from January 2015 to June 2015, we plan to pursue the ongoing R&D on individual aspects of the new ideas for the EIC-GEM chamber. The key element of this works is the continuation of the collaboration with Temple University

and Florida Tech to finalize the design drawings and submit the Gerber files to both US based Tech Etch as well as CERN PCB workshop for final review and validation. We are going to work on the design of the EIC u/v readout board in collaboration with the CERN PCB workshop as well as the support frames for the GEM foil. We plan to finalize the design of the complete FT Triple GEM module for the next funding cycle.
We are also planning to complete the analysis of the FTBF test beam data from the first EIC prototype and submit a paper to NIM or TNS on both the construction and the performance of the prototype.

Yale University:

3-Coordinate GEM
Further effort will be devoted to completing the analysis and publishing the results in the coming period.

Hybrid Gain Structure for TPC readout – 2 GEM plus Micromegas
Measurements will continue on different operating conditions of the 2-GEM+MMG gain structure. These will include for example further studies of different gas mixtures. It is known that the use of heavier hydrocarbons (C_4H_{10}) significantly improves the stability of MMG. A heavier ion may not be desirable for high rate environments however it may be acceptable for an electron-ion collider.
Studies on reducing the energy in a MMG discharge will continue. We have in hand interconnect boards implementing the "Floating Strip" circuit [1] that will allow us to study the behavior of this circuit. The circuit should provide spark protection for electronics as well as reducing the energy in a discharge, the region affected by the discharge and the recovery time.
Significant progress has been made recently in the use of resistive materials to reduce the discharge rate and energy in MMG. We will test a new idea to use a resistive plane to limit discharge energy and also improve charge sharing.

[1] https://indico.cern.ch/event/245535/session/4/contribution/5/material/slides/0.pdf

What are critical issues?

Brookhaven National Lab:

- Complete the final design of TPC/Cherenkov prototype detector
- Construct the TPC/Cherenkov prototype and test it in the lab
- Test the TPC/Cherenkov prototype in the test beam
- Identify suitable readout electronics for the TPC portion of the detector

Florida Tech:

Tech-Etch cannot produce 1m-class GEM foils unless they upgrade their existing production line. It is critical to the EIC FT project to support the development of larger GEM foil production facilities at this company. Upon our instigation, Tech-Etch has produced a full formal cost estimate for such an upgrade. They estimate a total investment of $200k, roughly evenly split between equipment cost and labor cost. We plan to request FY16 EIC R&D funds in June 2015 for a sizeable order of large EIC FT foils from TechEtch that will include such NRE costs. The order and corresponding funding requests would be shared roughly equally between the three FT groups (Florida Tech, Temple U., UVa). Such an investment will benefit not only the EIC project, but all U.S. universities and national labs by opening up a domestic source of large GEM foils.
The SRS electronics in our group have begun to age so some of them are behaving abnormally. We need to get new SRS electronics as soon as possible.

Stony Brook University:

Finalizing the studies for a charge division by means of dispersion scheme so that a suitable readout board can be produced and further tested.

University of Virginia:

Domestic production of large area GEM foil is a critical issue for the R&D effort toward GEM-based EIC Forward tracker. Tech Etch a US company has so far been the only other supplier, other than CERN workshop, capable of producing high quality large GEM foil but their current capability is limited to roughly (50×50 cm^2) well below the size required for EIC FT GEMs. Tech Etch has shown that they are able to meet the size required for EIC with an upgrade of their equipment and production capability. It is crucial for the EIC FT program that we support Tech Etch company for domestic production of large GEM foils and we are planning, together with the group at Florida tech and Temple University to make a joint FY16 EIC R&D funds request in June 2015 for the order of a roughly 20 large size GEM foils to Tech Etch as part of the program to support the development of GEMs by Tech Etch.

Yale University:

The critical issues continue to be methods for producing a robust TPC gain structure with good energy resolution and low ion feedback.

Additional information: **Budget etc.**

Brookhaven National Lab:

We are not requesting any additional funds at this time, but we expect to require additional funding for FY16. This will include funding to finish the construction of the TPC/Cherenkov prototype and test it in the lab. We will also need funds to upgrade our VUV spectrometer, which we need to study the photosensitive GEM portion of the detector. This funding has been deferred for several cycles but we will now need these funds in FY16. We also plan to do a beam test with the prototype in FY16 and will be requesting funding for this test. We expect to ask for $60K in funding to cover these items ($15K parts & supplies + $15K beam test + $10K optics = $40K x 1.5 overhead = $60K.)

Florida Tech:

We are not requesting any additional funds at this time, but we are anticipating to request funding for personnel (EIC post-doc Aiwu Zhang, 3rd year, ~$93k fully loaded) for FY16.
Together with UVa and Temple U., we anticipate placing an order for large GEM foils to Tech-Etch in FY16 that would incorporate substantial NRE cost because TechEtch needs to upgrade their production facility. If the cost are equally shared among the three FT groups, we'd anticipate a funding request of $50-70k per institution for FY16 for this purpose. In addition, we plan on requesting $10k in operating funds (gas, electronics) at Fl. Tech for FY16.
To summarize, we expect to ask for $153-173K in funding to cover the following:
$93K post-doc salary + $50-70K TechEtch GEMs + $10K operation = $153-173k.

Stony Brook University:

We are planning to test a new readout scheme via resistive anode charge sharing at a test-beam facility in FY16. We estimate these costs to be around $30k including material and overhead and will ask for this amount in the next round of proposals.

University of Virginia:

We are also planning to request additional FY16 EIC R&D funds at UVa to support build the second EIC GEM prototype to implement and test the ideas that we described in this report. This support funds that we anticipate to be in the range of 25 to 40 k$ will be used for the GEM parts such as support frames, custom stretching device.

Yale University:

N/A